



Synthesis and characterization of cellulose based graft copolymers with binary vinyl monomers for efficient removal of cationic dyes and Pb(II) ions

Rajesh Kumar^{1,2} · Rajeev Kr. Sharma³ · Anirudh P. Singh²

Received: 29 December 2018 / Accepted: 12 April 2019 / Published online: 11 May 2019
© The Polymer Society, Taipei 2019

Abstract

Cellulose grafted with 2-acrylamido-2-methylpropane sulfonic acid (AASO₃H) and binary comonomer acrylonitrile (AN) were synthesized and characterized by FTIR, XRD, SEM, TGA/DTA and swelling studies. Adsorption parameters like contact time, temperature, pH and concentration were optimized for maximum adsorption of organic dyes and Pb(II) ions. Dye adsorption behavior studied for cationic malachite green (MG) and crystal violet (CV) dyes followed the order Cell-g-AASO₃H > Cell-g-AASO₃H-co-AN > cellulose. Order for adsorption of dyes were reported as MG > CV. Pseudo-second-order model is best-fitted with the experimental data and adsorption capacity from Langmuir adsorption isotherm for MG, and CV were 61.46 and 55.71 mg.g⁻¹ respectively, for Cell-g-AASO₃H. Percent uptake capacities followed the order Cell-g-AASO₃H-co-AN > Cell-g-AASO₃H > cellulose for Pb(II) ions. Maximum adsorption capacities for Pb(II) ions from Langmuir adsorption isotherm were 154.32 and 181.49 mg.g⁻¹ for Cell-g-AASO₃H and Cell-g-AASO₃H-co-AN, respectively.

Keywords Graft copolymer · Characterization · Dye adsorption · Pb(II) sorption

Introduction

The release of highly toxic and poisonous dyes and heavy metal ions from the textile, dyeing, printing, food, pharmaceutical, cosmetic, and paint industries into the water bodies is of major concern nowadays. Organic dyes are generally non-biodegradable and accumulate in the water bodies. Due to strongly visible light absorption properties, these dyes increase the biological and chemical oxygen demand, change the pH and color of the water, which

drastically affect the growth of flora and fauna [1]. It has been reported that these dyes have highly adverse carcinogenic, mutagenic, cytotoxic and genotoxic effect in addition to less drastic skin disease, allergic reactions and respiratory problems [2]. Photo-catalytic degradation, sonochemical degradation, biodegradation, electrochemical degradation, chemical coagulation-flocculation, chemical precipitation, ultrafiltration, adsorption on activated charcoal/carbon have been reported as traditional methods for the removal of toxic dyes from aqueous solution [3]. Among all the reported techniques for the removal of toxic dyes from the industrial effluent, solid phase extraction have been a benchmark due to its low cost, easy applicability, and recyclability [4]. The need of the hour is to thus develop highly efficient biodegradable super-absorbent materials for wastewater treatment applications.

Cellulose is a pre-eminent biopolymer comprising β-D-anhydroglucopyranose units linked through covalent C₁-C₄ β-glycosidic linkages to form long straight chain fibrous macromolecules. The composition of this incredible biopolymer in different lignocellulosic biomasses varies from species to species. Different physical, chemical, biological, and physicochemical methods for the extraction of pure cellulose, from lignocellulosic biomass, are reported

Electronic supplementary material The online version of this article (<https://doi.org/10.1007/s10965-019-1790-9>) contains supplementary material, which is available to authorized users.

✉ Rajeev Kr. Sharma
rksharma_75@yahoo.co.in

¹ Post Graduate Department of Chemistry, Jagdish Chandra DAV College, Dasuya, Punjab 144205, India

² I.K. Gujral Punjab Technical University, Kapurthala-Jalandhar Highway, Kapurthala, Punjab 144601, India

³ Post Graduate Department of Chemistry, DAV College, Jalandhar, Punjab 144008, India

and well reviewed in the literature [5–8]. Due to the presence of three hydroxyl groups (–OH) at C₂, C₃ and C₆ atoms of each β-D- anhydroglucopyranose units of cellulose, its properties can further be improved, either through chemical modification [9, 10] or through the formation of more significant graft cellulose copolymers [11]. Graft copolymers of cellulose have been reported for heavy metal ion sorption from industrial effluents [12–14], dye adsorption from textile industry [15–17], controlled drug delivery [18, 19], enzyme immobilization [20], antimicrobial food packaging materials [21, 22] and, component modification of secondary Li-ion batteries [23]. The performance of graft copolymers of cellulose is highly dependent upon the degree of crystallinity, specific surface area, the degree of polymerization of the grafted monomers onto cellulose, the nature of the functional groups present on the grafted monomers and co-monomers, hydrophilicity and hydrophobicity etc.

Malachite green (MG) and crystal violet (CV) dyes are triarylmethane cationic dyes, widely used in as histological stain. Both the dyes are water-soluble and non-biodegradable in nature which pose serious carcinogenic, mutagenic, and cytotoxic effects on mammalian cells. Many cellulose based adsorbents have been reported in the literature for the adsorption of these toxic dyes. M. Ghaemy et al. reported the preparation of adsorbent nanoparticles based on treated low-value agricultural by-product rice husk and poly(methylmethacrylate-co-maleic anhydride) for the removal of CV dye from water [24]. S. Chowdhury and coworkers developed low-cost adsorbents from NaOH-modified rice husk for removal of CV [25] and MG dyes [26]. Cellulose modified with glycidyl methacrylate and sulfosalicylic acid was reported as a better adsorbent of CV dye than native cellulose [27]. Cellulose modified with maleic and phthalic anhydride were synthesized and reported better adsorbents than pristine cellulose for the removal of MG from aqueous solution by Zhou et al. [28]. Zheng et al. [29] and Ruan et al. [30] removed CR dye using composite thin films and beads, respectively composed of chitosan and 2,3-dialdehyde cellulose. Wang et al. synthesized polyacrylamide grafted quaternized cellulose to remove Congo red and Eriochrome blue SE anionic dyes from aqueous solution [31]. Carboxylated cellulose nanocrystals were also reported for the effective adsorption of cationic dyes like CV, MG and methylene blue [32].

Chauhan and coworkers have developed grafted cellulose extracted from forest waste pine needles with various vinyl monomers to develop hydrogels which were sensitive to change in temperature, pH, ionic strength and selectivity to metal ions [33, 34]. Interpenetrating networks based on extracted cellulose grafted with methacrylamide in presence of N,N-methylene bisacrylamide were

synthesized and used in sorption of Fe(II), Cu(II) and Cr(VI) ions [35]. Cellulosic adsorbent were synthesized by γ-initiated grafting of poly(glycidyl methacrylate) onto cellulose filter paper for Cd(II), Pb(II) and Cu(II) removal from aqueous media [36]. Natural cellulosic fibers like cotton grafted with glycidyl methacrylate and methacrylic acid using gamma irradiation were used for sorption of Co(II) ions [37]. Cellulose cotton fibers were also modified through graft copolymerization of polyacrylonitrile for removal and extraction of Au(III), Pd(II) and Ag(I) precious metal ions [38]. Cellulose grafted with 2-hydroxy methacrylate and its binary monomer mixtures with acrylamide, acrylic acid, and acrylonitrile were investigated for sorption of Fe(II), Cu(II) and Cr(VI) ions [39]. Hajeeth and et al. reported the extraction of cellulose from sisal fiber and grafted it with acrylic acid to develop adsorbent for Cu(II) and Ni(II) ions [40] and grafted acrylonitrile for sorption of Cr(VI) ions from aqueous solution [41]. Grafting of acrylic acid and 2-acrylamido-2-methyl propane sulphonic acid onto cellulose in the presence of crosslinking agent of N,N-methylene bisacrylamide were found to be selective for the removal of Pb(II) over Cu(II) and Cd(II) ions [42]. Cellulose was extracted from peanut hulls, soybean shells and grape fruit peels and then copolymerized with epichlorohydrin and ethylenediamine used as potential low-cost and high efficient adsorbents for removal of lead ions from wastewater [43].

2-Acrylamido-2-methylpropane sulfonic acid (AASO₃H) is a hydrophilic, sulfonic acid acrylic monomer and consists of geminal dimethyl substituents. The protonation – deprotonation properties (–SO₃H → –SO₃[–]) of the sulfonic acid (–SO₃H) moiety in the medium makes it an attractive site for the adsorption of a variety of adsorbate materials including toxic metal ions and hazardous non-biodegradable dyes. The hydrophilic nature of the monomer also makes it a suitable candidate to perform its grafting on to natural polysaccharides like cellulose, starch, chitin, and chitosan etc. in non toxic aqueous media. Further, acrylonitrile (AN) is also a vinyl monomer with a nitrile (–C≡N) pendent group. Un-hydrolyzed –C≡N group as well as amide group (–CONH₂), formed after the acidic or alkaline hydrolysis act as potential sites for the attraction of different varieties of adsorbates similar to AASO₃H.

In context to properties of AASO₃H and AN copolymers, herein we reported a fast, facile and low-cost synthesis of graft copolymers of AASO₃H and its binary comonomer mixture with AN onto cellulose extracted from rice husk. >The morphological, structural, compositional, thermal, and vibrational properties of the synthesized materials were characterized by different characterization techniques. Graft copolymers were investigated for their potential applications for adsorption of MG, CV dyes and Pb(II) ions from aqueous solution.

Materials and methods

Materials

For the extraction of cellulosic fibers, agricultural residue, rice husk was purchased from a local rice mill. For the extraction and chlorine-free bleaching of the cellulose, sodium peroxide (Na_2O_2), hydrogen peroxide (H_2O_2), ethanol, dimethylformamide (DMF), acetone and sodium hydroxide were purchased from CDH fine chemicals, India. 2-acrylamido-2-methylpropane sulfonic acid (AASO₃H; HiMedia Lab. Pvt., Ltd. Mumbai, India), potassium persulfate (KPS, $\text{K}_2\text{S}_2\text{O}_8$; Paskem Fine Chemicals, India), N,N'-Methylenebisacrylamide (N,N'-MBA; HiMedia Lab. Pvt., Ltd. Mumbai, India) were purchased for the synthesis of cellulose grafted copolymer. Co-monomer AN was supplied by SD Fine Chemicals Ltd., Mumbai, India. All the chemicals were of analytical grade and used as received without any further purifications. MG and CV dyes were purchased from Loba Chemicals, India. For sorption studies of Pb(II) ions, $\text{Pb}(\text{NO}_3)_2$ was purchased from SD Fine, India. All the solutions for batch experiments were prepared in ultrapure water obtained from BIO-AGE Water Purifier System, model Direct Ultra TUVF-5.

Extraction of cellulose from rice husk

A greener, total chlorine free and ultrasonic physicochemical process of extraction and purification of cellulose from rice husk, as explained by Sharma et al. [44], was employed. Briefly, the initial step involves the treatment of the rice husk with a concentrated aqueous alkali solution for the duration of 6 h at 80 °C in round bottom flask in order to completely dissolve lignin and silica. After alkali pretreatment, the product obtained was thoroughly washed with distilled water, filtered and dried. The dried product was subjected to mechanical treatment followed by bleaching. A sonolytic technique was applied for the bleaching of cellulose using $\text{Na}_2\text{O}_2/\text{H}_2\text{O}_2$ in alkaline medium, as a chlorine-free bleaching agent.

Synthesis of cellulose based graft copolymers

Optimization of the different grafting reaction conditions for AASO₃H onto 1 g of extracted cellulose in the presence of N,N'-MBA cross-linker was carried out by KPS initiated free radical mechanism. The grafting reaction scheme was designed in such a way that one reaction parameter was varied for a set of grafting reactions keeping the other reaction parameters constant (Table 1). Various grafting reaction parameters optimized to obtain maximum graft yield were nature of the solvent, solvent volume, monomer concentration, cross-linker concentration, initiator concentration, grafting

temperature and reaction time. Methanol-acetone mixture was used as an extraction solvent for the separation of graft copolymers and homopolymers of AASO₃H. The percent grafting (P_g) and percent grafting efficiency (GE) were calculated using Eqs. 1 and 2, respectively [45].

$$P_g = \frac{W_2 - W_0}{W_0} \times 100 \quad (1)$$

$$GE = \frac{W_2 - W_0}{W_1} \times 100 \quad (2)$$

Where, W_0 = Weight of ungrafted cellulose, W_1 = Weight of monomer, and W_2 = Weight of grafted copolymer.

At the optimized grafting reaction conditions for grafting of AASO₃H onto cellulose binary comonomer, AN was grafted at five different concentrations (Table 2). Homopolymers poly(AN) were removed by using DMF solvent.

Characterization of graft copolymers

Characterization of pristine cellulose, Cell-g-AASO₃H, and Cell-g-AASO₃H-co-AN for structural, morphological, crystalline, transmittance and thermal properties was carried out by different techniques. Morphological and structural properties were studied by field emission scanning electron microscopic (SEM) analysis (Jeol, JSM-6100 at an accelerating voltage of 20 kV). X-ray diffraction (XRD; PAN analytical, Netherlands, Rigaku Rota-Flex operating with Cu-K α radiation, 45 kV) patterns were studied between diffraction angles (2θ) ranging from 10–80°. Fourier transform infrared (FTIR; Thermo Nicolet Model 6700 spectrophotometer) spectra of the samples were analyzed through KBr pelletization in 400–4000 cm^{-1} range. Thermal-gravimetric (TGA) and differential thermal analysis (DTA) (Hitachi STA7200 Thermal Analyser; simultaneous TG/DT model) were carried out at 30–750 °C temperature. Finally, swelling properties of the cellulose-based copolymers were also studied in buffer solutions with pH values 2.2, 7.0 and 9.4. Accurately weighed (100 mg) polymer sample was placed in 10.00 mL of the buffer solution for different time intervals. After a suitable time interval, surface water was removed from the swollen polymer and polymer was dried by softly pressing it between the folds of filter paper. The increase in weight of the swollen copolymer was recorded. Percent swelling (P_s) was calculated using Eq. 3 [46].

$$P_s = \frac{W_s - W_d}{W_d} \times 100 \quad (3)$$

Where, W_s = Weight swollen copolymer, and W_d = Weight of dried copolymer.

Table 1 Effect of reaction conditions for optimum grafting of AASO₃H onto 1 g of cellulose

Solvent	Vol. (mL)	[AASO ₃ H] × 10 ⁻² (mol L ⁻¹)	[KPS] × 10 ⁻² (mol L ⁻¹)	N,N'-MBA (in g)	Temp (° C)	Time (min)	P _g (%)	GE (%)
Effect of nature of the solvent								
CCl ₄	10.0	48.251	9.25	0.1	60	5	6.00	6.00
Benzene	10.0	48.251	9.25	0.1	60	5	3.00	3.00
H ₂ O	10.0	48.251	9.25	0.1	60	5	78.0	78.0
Dioxane	10.0	48.251	9.25	0.1	60	5	12.0	12.0
Acetone	10.0	48.251	9.25	0.1	60	5	28.0	28.0
Effect of the amount of solvent								
H ₂ O	10.0	48.251	9.25	0.1	60	5	78.0	78.0
H ₂ O	15.0	32.251	6.166	0.1	60	5	38.0	38.0
H ₂ O	20.0	24.125	4.625	0.1	60	5	29.0	29.0
H ₂ O	25.0	19.30	3.699	0.1	60	5	11.0	11.0
Effect of monomer concentration								
H ₂ O	10.0	24.126	9.25	0.1	60	5	30.0	60.0
H ₂ O	10.0	48.251	9.25	0.1	60	5	78.0	78.0
H ₂ O	10.0	72.376	9.25	0.1	60	5	94.0	62.67
H ₂ O	10.0	96.501	9.25	0.1	60	5	152.0	76.0
H ₂ O	10.0	120.627	9.25	0.1	60	5	131.0	52.4
Effect of initiator concentration								
H ₂ O	10.0	96.501	4.624	0.1	60	5	118.0	59.0
H ₂ O	10.0	96.501	9.25	0.1	60	5	150.0	75.0
H ₂ O	10.0	96.501	13.87	0.1	60	5	188.0	94.0
H ₂ O	10.0	96.501	18.50	0.1	60	5	249.0	124.5
H ₂ O	10.0	96.501	23.13	0.1	60	5	223.0	111.5
Effect of reaction temperature								
H ₂ O	10.0	96.501	18.50	0.1	30	5	10.0	5.0
H ₂ O	10.0	96.501	18.50	0.1	40	5	32.0	16.0
H ₂ O	10.0	96.501	18.50	0.1	50	5	139.0	69.5
H ₂ O	10.0	96.501	18.50	0.1	60	5	249.0	124.5
H ₂ O	10.0	96.501	18.50	0.1	70	5	232.0	116.0
Effect of reaction time								
H ₂ O	10.0	96.501	18.50	0.1	60	3	190.2	95.1
H ₂ O	10.0	96.501	18.50	0.1	60	4	224.2	112.1
H ₂ O	10.0	96.501	18.50	0.1	60	5	249.0	124.5
H ₂ O	10.0	96.501	18.50	0.1	60	6	218.4	109.2
H ₂ O	10.0	96.501	18.50	0.1	60	7	194.6	97.3
Effect of cross-linker concentration								
H ₂ O	10.0	96.501	18.50	0.05	60	5	145.0	72.5
H ₂ O	10.0	96.501	18.50	0.10	60	5	249.0	124.5
H ₂ O	10.0	96.501	18.50	0.15	60	5	212.0	106.0
H ₂ O	10.0	96.501	18.50	0.20	60	5	183.0	91.5
H ₂ O	10.0	96.501	18.50	0.25	60	5	169.0	84.5

Dye adsorption applications

The adsorption behavior of cellulose and graft copolymers for both the cationic dyes was studied. Batch experiments were

conducted using 0.05 g of the graft copolymer as adsorbent for 50 mL dye solutions of different concentrations. After specific time intervals, dye solution aliquots were withdrawn and the concentration of the remaining dye was determined at the

Table 2 Grafting of binary monomer mixture AASO₃H and AN onto cellulose

S. N.	[AASO ₃ H] × 10 ⁻² (mol L ⁻¹)	[AN] × 10 ⁻² (mol L ⁻¹)	P _g	GE
1	96.501	0.00	249.0	124.5
2	96.501	48.251	193.0	96.50
3	96.501	96.501	220.0	110.0
4	96.501	144.752	227.0	113.5
5	96.501	193.002	230.0	115.0
6	96.501	241.253	267.0	133.5

characteristic wavelength (λ_{\max} = 615 and 588 nm, for MG and CV respectively) with the help of UV – Vis spectrophotometer (Systronics–2202, Double beam spectrophotometer) at calibrated curves. This optimized time was used for all the subsequent experiments to evaluate the adsorption performance of Cell-g-AASO₃H copolymers. In order to improve the reliability and validity of the adsorption data, all the experiments were performed in triplicate and the average of the results is used for analysis.

Effects of the initial dye concentration, contact time and temperature (20–40 °C), on the adsorption capacities of the synthesized Cell-g-AASO₃H and Cell-g-AASO₃H-co-AN were studied at optimized conditions, and results were compared with adsorption capacities of extracted cellulose as a reference. The nature of the dyes and the pH of the solution have a significant effect on the adsorption. Thus, the effect of pH (2.2, 7.0 and 9.4) on the adsorption performances of Cell-g-AASO₃H and Cell-g-AASO₃H-co-AN copolymers were studied at optimized conditions of time, temperature, and concentration of the dye solutions. Amount of dye adsorbed (q_t – mg/g) and percent dye removal (D_e – %), were calculated as per Eqs. 4 and 5.

$$q_t = \frac{C_o - C_t}{W_d} V \quad (4)$$

$$D_e = \frac{C_o - C_t}{C_o} \times 100 \quad (5)$$

Where, C_o = Initial dye concentrations (ppm), C_t = Dye concentrations (ppm) in the solution after time ‘t’ (min), V = Volume of the dye solution (L) and, W_d = Weight of adsorbent taken (g).

Metal ions sorption applications

Batch experiments were also conducted to evaluate the sorption capacities of pure cellulose, Cell-g-AASO₃H and Cell-g-AASO₃H-co-AN copolymers towards the sorption of Pb(II) metal ions from the medium. Accurately weighed 0.05 g of the sorbent was immersed in 50 mL aqueous solution of Pb(II) ions of known concentration. The concentration of Pb(II) ions after sorption was estimated through back titration using standardized EDTA solution and Eriochrome black T as an indicator [47]. All the batch experiments were repeated thrice to calculate the mean values. The sorption amount ‘q’ and

percent uptake (P_u) of the Pb(II) ions sorbed were calculated using Eqs. 6–7, respectively.

$$q = \frac{C_o - C_t}{W_d} V \quad (6)$$

$$P_u = \frac{C_o - C_t}{C_o} \times 100 \quad (7)$$

Where, C_o = Initial concentration of metal ions, C_t = Concentration of the Pb(II) ions left in solution after time ‘t’, W_d = Weight of the copolymer (g), and V = Volume of the of the Pb(II) ion solution taken.

Results and discussion

Optimization of grafting parameters of AASO₃H onto extracted cellulose

Effect of nature and amount of solvent

Solvent acts as a medium for the transportation and diffusion of the monomer units to the vicinity of the –OH groups of cellulose backbone. Generation of the free radicals, wetting, and swelling of the cellulose backbone, chain transfer, H-abstractions, control of the chain termination effects, etc. are some of the other important factors which depend upon the nature of the solvent. Thus, the proper selection of the solvent is critical. The solvent effect on P_g and percent GE was studied in 10.00 mL of CCl₄, benzene, water, dioxane, and acetone, in the presence of monomer; [AASO₃H] = 48.251 × 10⁻² mol L⁻¹, initiator; [KPS] = 9.25 × 10⁻² mol L⁻¹, crosslinker; [N,N'-MBA] = 0.1 g (10 wt% of monomer, AASO₃H), grafting temperature = 60 °C and grafting time = 5 min. Under these grafting conditions, maximum P_g and percent GE were recorded in the water (Table 1). The order for P_g and GE in different solvents was: Water > Acetone > dioxane > CCl₄ > Benzene. The results may be attributed to the excellent solubilities of the monomer, free radical initiator, and crosslinker, fast diffusion of the monomer, maximum swelling of the cellulose backbone, negligible chain transfer constant, and minimum wastage of the monomer in water as compared to other solvents under study.

The reasonable change was observed in the P_g and percent GE of the copolymers when the volume of the water was increased from 10 mL to 25 mL. All other parameters were kept constant (Table 1). P_g values of 78, 38, 29, and 11 were observed for 10, 15, 20 and 25 mL of water as a solvent, respectively. A large volume of water makes the reacting species (monomer) less accessible to cellulose backbone which results in homopolymer formation [48]. Volume less than 10 mL was found insufficient for the proper wetting of the cellulose backbone and dissolution of other chemical reagents, hence no proper results could be inferred. As maximum P_g and percent, GE was recorded for 10 mL of water, all the subsequent experiments were performed using the same optimized volume.

Effect of monomer and initiator concentration

In order to check the effect of the concentration, grafting experiments were conducted at different concentration of AASO₃H varying from $24.126 \times 10^{-2} \text{ mol L}^{-1}$ to $120.627 \times 10^{-2} \text{ mol L}^{-1}$ at KPS concentration of $9.25 \times 10^{-2} \text{ mol L}^{-1}$, N,N'-MBA amount of 0.1 g, temperature 60 °C, grafting reaction time 5 min and at optimum solvent volume (10 mL). The increase in the P_g and percent GE was observed with the initial increase in the monomer concentration up to $96.501 \times 10^{-2} \text{ mol L}^{-1}$, maximum P_g , and percent GE were recorded as 152.0 and 76.0 respectively. At higher AASO₃H concentrations, the possibilities of coupling of grown macro-radicals accelerate the mutual chain termination, thereby forming homopolymers rather than grafted copolymers.

Free radical initiators can either increase the number of grafts per cellulose backbone or can add monomer units to the already grafted chains. For these two processes to operate, a proper concentration of the free radicals is required and hence the chemical initiator is necessary for the reaction mixture. Herein, the effect of change in KPS concentration ($4.624 \times 10^{-2} \text{ mol L}^{-1}$ to $23.13 \times 10^{-2} \text{ mol L}^{-1}$) on P_g and percent GE was studied. It is apparent from Table 1 that at with increase in KPS concentration to $18.5 \times 10^{-2} \text{ mol L}^{-1}$ maximum P_g , and percent GE were recorded as 249.0 and 124.5 respectively. But with further increase in concentration of initiator, it did not increase the P_g and percent GE. It is due to the fact that at higher KPS concentration, either homopolymerization is induced or coupling of the grown polymer chains takes place [49]. These two attributes result in the decreased grafting yield.

Effect of temperature and time

For temperature optimization, grafting of AASO₃H onto cellulosic backbone was carried out between 30 and 70 °C, by keeping all other influencing parameters constant. As the

grafting temperature was increased from 30 °C to 60 °C, P_g was increased significantly from 10 to 249. After that, a decrease in P_g was reported as the grafting temperature was increased to 70 °C. Low grafting yield, at a temperature lower than the optimum temperature, is due to the lower rate of decomposition of the KPS initiator and retarded diffusion rates of monomers to the active sites, whereas at high temperature, the graft copolymerization occurs with poor selectivity and various other side reactions such as hydrogen abstraction, chain transfer, and homopolymerization reactions become operative [39].

With the increase in the reaction time from 3 min to 5 min the P_g increased from 190.2 to 249.0 and after this, a further increase in the grafting time up to 7 min, a significant decrease was recorded for the P_g as well as GE (Table 1). This may be attributed to the partial decomposition of grown polymer chains over the cellulose backbone [45, 46, 50].

Effect of cross-linker concentration

The amount of N,N'-MBA was varied from 2.5–12.5 wt% with respect to the amount of the cellulose backbone by maintaining all other grafting parameters constant. Maximum P_g and percent GE were 249.0 and 24.5, respectively for 10 wt% of N,N'-MBA. Beyond 10 wt%, both P_g and GE were decreased (Table 1). As the concentration of the N,N'-MBA cross-linker increases, large number of cross-linking points are formed which promote the formation of network structures rather than grafting of the vinyl monomers [51, 52].

Synthesis of Cell-g-AASO₃H-co-AN copolymers

In order to increase the density of functional groups, AN as binary comonomer, was grafted onto 1 g cellulose at the optimized grafting conditions evaluated for grafting of AASO₃H i.e. [AASO₃H] = $96.501 \times 10^{-2} \text{ mol L}^{-1}$, initiator; [KPS] = $18.5 \times 10^{-2} \text{ mol L}^{-1}$, cross-linker; [N,N'-MBA] = 0.1 g (5 wt% of monomer AASO₃H), grafting temperature = 60 °C and grafting time = 5 min in 10 mL of water as solvent. Only the concentrations co-monomer AN was varied from 0.5 to 2.5 M ratios with respect to the molar concentration of AASO₃H (Table 2). The grafting parameters like P_g and percent GE were continuously increased with increase in the concentration of AN. Maximum P_g and GE values of 267.0 and 133.5, respectively were calculated for Cell-g-AASO₃H-co-AN at 2.5 M ratios. However, for initial concentrations of AN i.e. 0.5–2.0 M ratios *w.r.t.* the molar concentration of AASO₃H, both P_g and GE for Cell-g-AASO₃H-co-AN copolymer were low as compared to Cell-g-AASO₃H copolymer. The fact may be attributed to the hydrophobic nature of the AN vinyl monomer. The simultaneous presence of the AN and AASO₃H monomers in the reaction medium increases the monomer molecules relative to the available

graft free radical sites, which results in competition for the active sites, thereby reducing P_g and GE. This further favors homopolymerization over graft copolymerization [53].

Characterization of the pure cellulose and grafted copolymers

SEM analysis

The morphological and structural properties of the pure cellulose, Cell-g-AASO₃H, and Cell-g-AASO₃H-co-AN were evaluated through SEM analysis. Long and individual bundled cellulose fibers with high aspect ratio and an average diameter of $6 \pm 1 \mu\text{m}$ were observed. Additionally, the raw cellulosic fibers have relatively smooth surfaces as compared to the cellulose grafted with unitary and binary monomers. Cell-g-AASO₃H displayed a thick flaky appearance, whereas the binary Cell-g-AASO₃H-co-AN copolymer displayed highly flaky, porous and lumpish appearance due to the grafting of AN monomer units (Fig. 1).

XRD analysis

The XRD spectrum for pure cellulose revealed diffraction peaks at diffraction angles $(2\theta) = 15.36^\circ$, 22.33° and 34.55°

which correspond to the (101), (002) and (004) diffraction planes, respectively. These are the characteristic peaks for I_β form of cellulose polymorphs [54]. The intensities for the peaks, corresponding to all the diffractions planes were decreased for Cell-g-AASO₃H and Cell-g-AASO₃H-co-AN copolymers (Fig. 2). The crystallinity index (C_I) values for all the samples were calculated using the maximum intensities corresponding to the crystalline region and the intensities at the minimum for the amorphous fraction according to the Segal method (Eq. 8) [55].

$$C_I = \frac{I_{(002)} - I_{am}}{I_{(002)}} \times 100 \quad (8)$$

Cell-g-AASO₃H and Cell-g-AASO₃H-co-AN showed lower crystallinity index values of 44.03 and 40.11%, respectively as compared to 68.33% crystallinity index for pure cellulose fibers (Table 3).

It is interesting to note that, the crystallinity indexes were decreased as the percent grafting of the copolymers was increased. Lower crystallinity index values for all the grafted cellulose fibers further indicate that there may be the disorientation of the cellulose crystals upon grafting of different monomer units onto cellulose fibers.

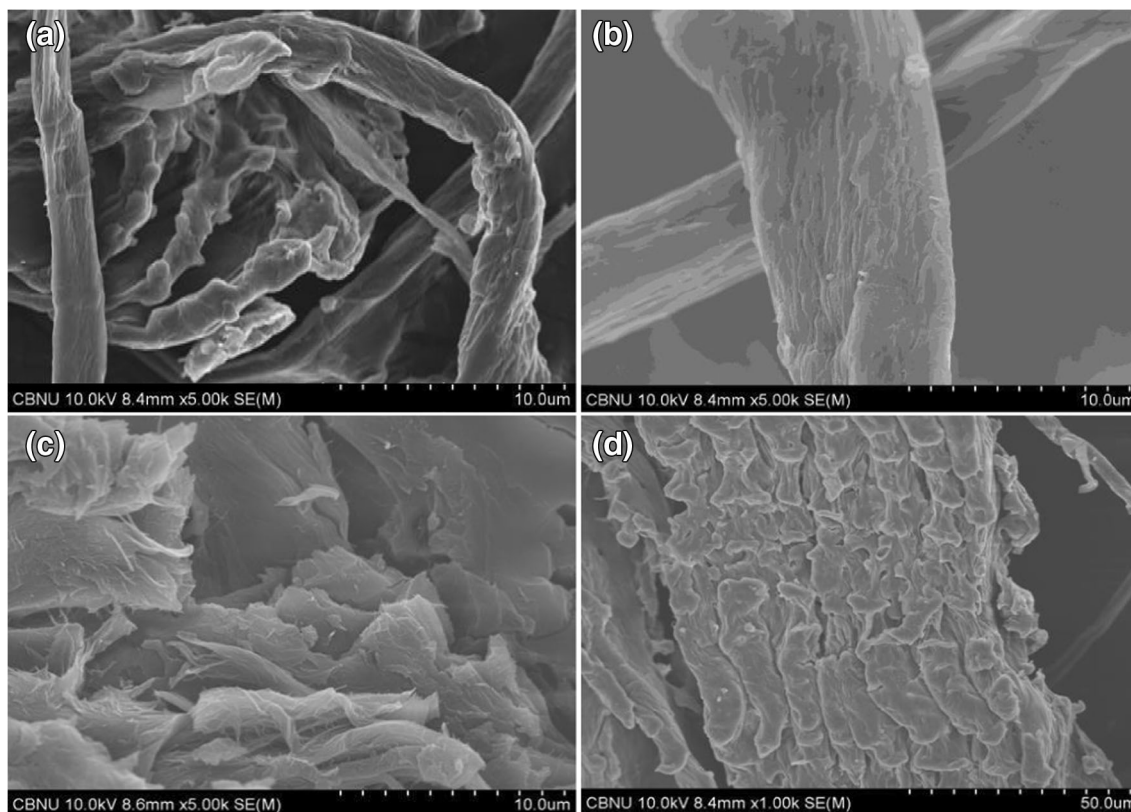
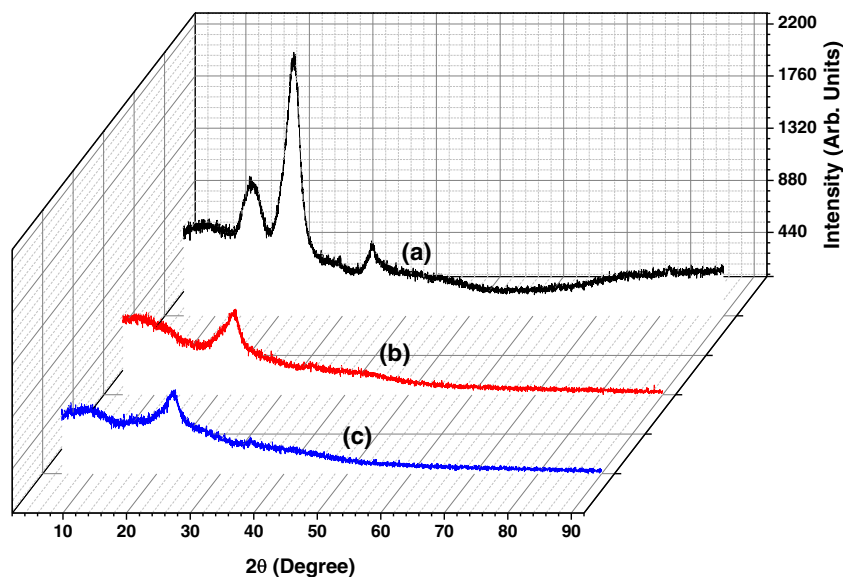


Fig. 1 SEM images for (a, b) pure cellulose extracted from rice husk, (c) Cell-g-AASO₃H and (d) Cell-g-AASO₃H-co-AN

Fig. 2 XRD spectra for (a) pure cellulose extracted from rice husk (b) Cell-*g*-AASO₃H and (c) Cell-*g*-AASO₃H-*co*-AN



FTIR analysis

The FTIR spectra for the pure cellulose, Cell-*g*-AASO₃H, and Cell-*g*-AASO₃H-*co*-AN copolymer were analyzed to ascertain the composition and grafting of the monomer units onto the cellulosic fibers. The FTIR peaks at 1637.8, 1430.8, 1320.6, 1163.7, 1057.8 and 897.0 cm⁻¹ are the characteristic peaks of the native cellulose (Fig. 3a) [44]. The peak at 1637.8 cm⁻¹ may be assigned to the bending vibrational modes for the inter and intra-molecular hydrogen bonded hydroxyl (-OH) groups and adsorbed water molecules. Weak peaks at 1430.8 and 1320.6 cm⁻¹ were attributed to the bending vibrational modes of the methylene group (δ -CH₂). An additional set of strong peaks present at 1163.7, 1057.8 cm⁻¹ corresponds to the glycosidic bond (C-O-C) of the cellulose backbone and O-H bending vibrational modes for the primary alcoholic groups. The peak around 897.8 cm⁻¹ corresponds to the C-O stretching vibrational mode of the saccharide units.

The FTIR spectrum of Cell-*g*-AASO₃H showed characteristics peaks for the AASO₃H moiety in addition to the normal cellulose backbone peaks. This confirms the grafting of the AASO₃H monomer units on to the cellulose backbone. Sharp and well-defined peak at 1640.3 cm⁻¹ is attributed to the >C=O moiety of the amide group, relatively low-intensity peak at 1549.1 cm⁻¹ is due to the N-H bending vibrational mode of amide group, very low-intensity peak at ~3000 cm⁻¹

is due to the stretching band of -OH moiety of the sulfonic acid (-SO₃H) group. Additional prominent peaks at 1153.6 and 1115.2 cm⁻¹ are also the characteristic peaks of the -SO₃H group (Fig. 3b). The peaks at 1369.4, 1031.7 and 619.0 cm⁻¹ may be attributed to C-N stretching vibration of the amide group as well as C-H bending modes of the methyl (-CH₃) group, S-O stretching vibrational modes of the -

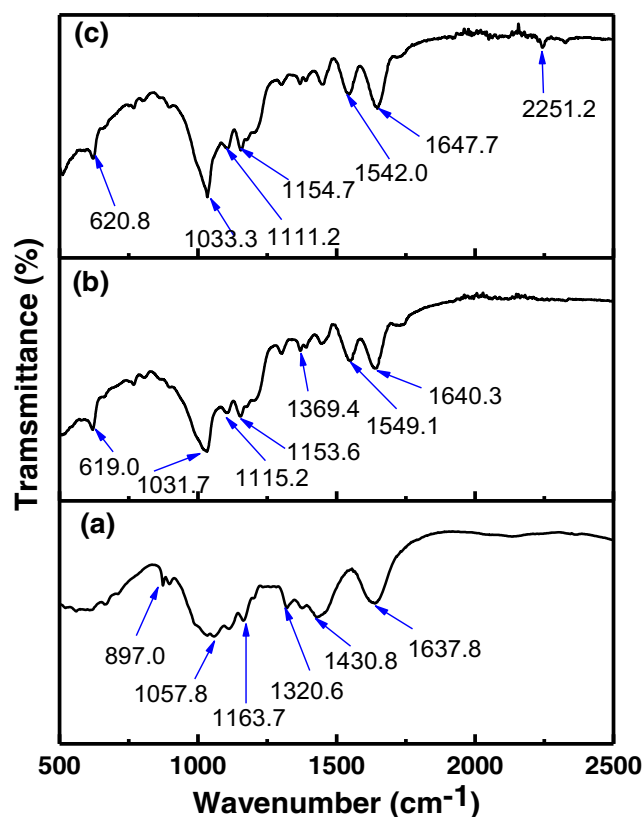


Fig. 3 FTIR spectra for (a) pure cellulose extracted from rice husk (b) Cell-*g*-AASO₃H and (c) Cell-*g*-AASO₃H-*co*-AN

Table 3 Crystallinity indexes for pure cellulose and various grafted copolymers

S.N.	Sample	P _g	I ₍₀₀₂₎	I _(am)	C ₁ (%)
1.	Pure cellulose	0.00	2291.37	725.74	68.33
2.	Cell- <i>g</i> -AASO ₃ H	249.0	791.40	442.91	44.03
3.	Cell- <i>g</i> -AASO ₃ H- <i>co</i> -AN	267.0	775.26	464.34	40.11

SO₃H, and C–S stretching vibrations, respectively. The presence of a low intensity but sharp peak at 2251.2 due to the C≡N stretching affirms the grafting of the AN monomer units in Cell-g-AASO₃H-co-AN grafted copolymer (Fig. 3c).

Thermal analysis

Cellulose thermogram shows single stage degradation up to 199.5 °C with 7.9% weight loss (Fig. 4a). From 199.5 to 368 °C sharp loss in weight of 71.4% is observed which can be attributed to the processes like depolymerization, decomposition of the glycosidic bonds (C–O–C) and dehydration [44]. Final decomposition temperature (FDT) is observed at 499.5 °C leaving 0.7% residue. In addition to a sharp exothermic peak at 338.4 °C, two low-intensity exothermic peaks at 377.6 and 439.5 °C can be seen in DTG thermogram of cellulose.

DTA thermogram for pure cellulose extracted from rice husk exhibits two prominent exothermic peaks at 390.4 °C and 442 °C. For Cell-g-AASO₃H graft copolymer, TGA thermogram shows a steep and continuous weight loss of 71.4% up to 500.8 °C which can be due to the degradation of sulfonic acid (–SO₃H) groups, decomposition of cellulosic backbone

resulting in the evolution of CO₂ molecules and the disintegration of the charred residue (Fig. 4b). FDT was recorded at 543.7 °C at which 16.6% residue is left. Higher FDT and more amount of residue left at FDT for Cell-g-AASO₃H copolymer confirm its greater stability than pure cellulose. DTG showed three exothermic peaks at 233.1 °C, 303.2 °C and 534.5 °C whereas the DTA thermograph of the Cell-g-AASO₃H graft copolymer exhibited only a single exothermic peak at 540.7 °C which can be assigned to the degradation –SO₃H groups of Cell-g-AASO₃H graft copolymer.

In the case of Cell-g-AASO₃H-co-AN, the TGA thermogram represents a marginal decrease of 10.5% weight up to 199.4 °C. A significant weight loss of 34.4% can be seen from 199.4 °C to 367.1 °C. After that 14.8% weight loss was recorded between 367.1 °C to 500.1 °C (Fig. 4c). FDT was even higher than the Cell-g-AASO₃H copolymer and was marked at 658.6 °C with 5.4% residue left. Thus it can be concluded that the introduction of AN comonomer in the grafting process increases the thermal stability of the graft copolymer. Exothermic peaks at 582.7 °C in DTA of Cell-g-AASO₃H-co-AN may be because of decomposition of (–SO₃H) groups of AASO₃H and –CN groups of AN comonomers. Three prominent exothermic peaks at 309.7 °C, 577.9 °C and

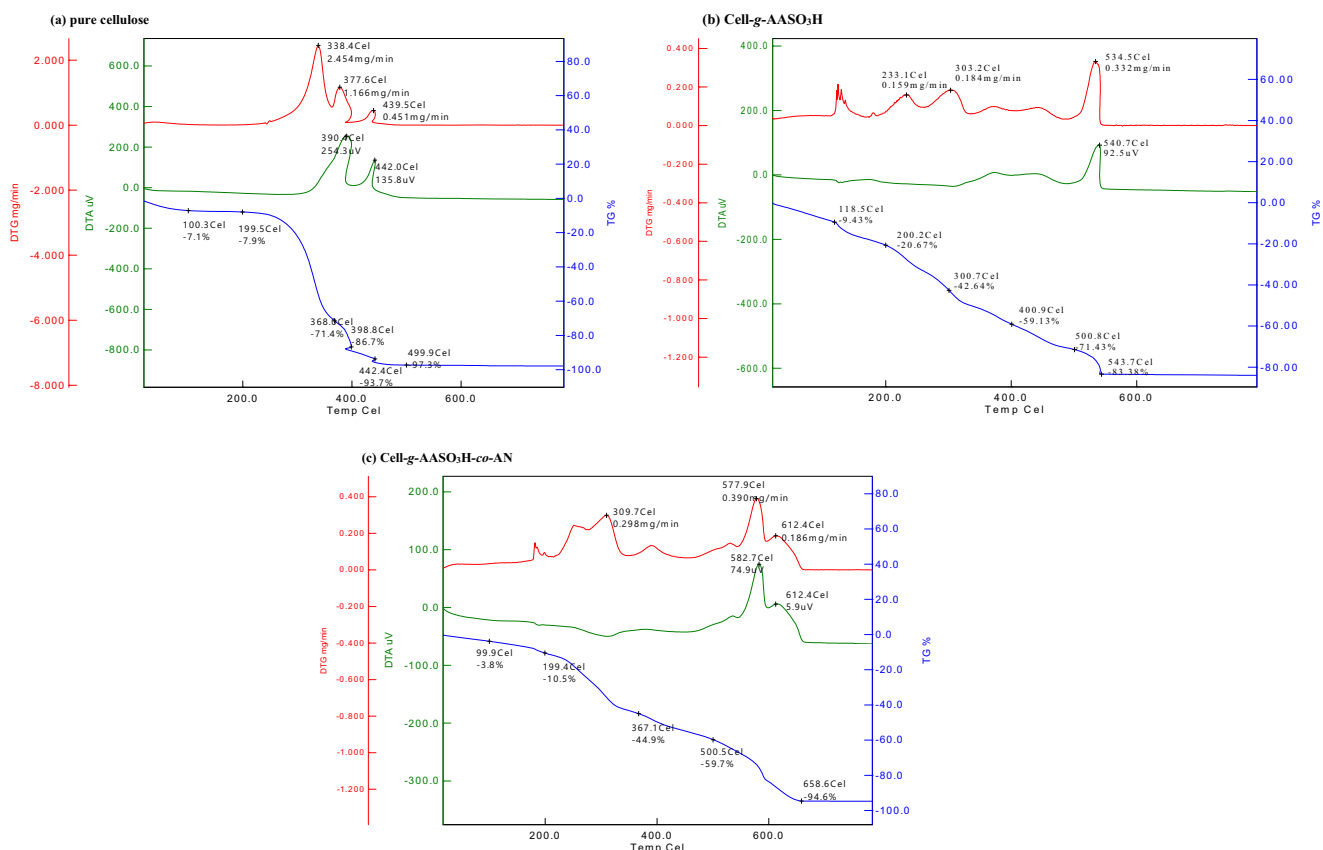


Fig. 4 Thermogravimetric spectra for (a) pure cellulose extracted from rice husk, (b) Cell-g-AASO₃H and (c) Cell-g-AASO₃H-co-AN

612.4 °C are observed in DTA of Cell-g-AASO₃H-co-AN which may also be because of the decomposition of $-C \equiv N$ groups of AN.

Swelling properties

Swelling properties of bare cellulose and its graft copolymers Cell-g-AASO₃H and Cell-g-AASO₃H-co-AN with maximum P_g (all 100 mg), under different pH conditions (2.2, 7.0 and 9.4) were compared. Under different pH conditions, Cell-g-AASO₃H showed maximum swelling as compared to the cellulose and Cell-g-AASO₃H-co-AN. All the samples attained maximum swelling within 2 h of the contact time (Fig. 5a–c). After that marginal change in swelling was observed. Figure 5d represents the P_s values for different adsorbents at 2.2, 7.0 and 9.4 pH after 24 h of the contact time. Ungrafted cellulose showed minimum P_s as compared to all the grafted copolymers. With the increase in the pH of the medium, however, the P_s values were increased.

Ungrafted cellulose showed maximum P_s of 29.4, 54.4 and 128 at 2.2, 7.0 and 9.4 pH values, respectively. P_s values for Cell-g-AASO₃H and Cell-g-AASO₃H-co-AN copolymers of cellulose followed the order 9.4 > 7.0 > 2.2. At pH 9.4 maximum P_s of 1942.9, 1339.3 and 128 was recorded for Cell-g-AASO₃H, Cell-g-AASO₃H-co-AN and cellulose respectively. The maximum rate of swelling at pH 9.4 is attributed to the sodium salt formation and hydrolysis of the nitrile group

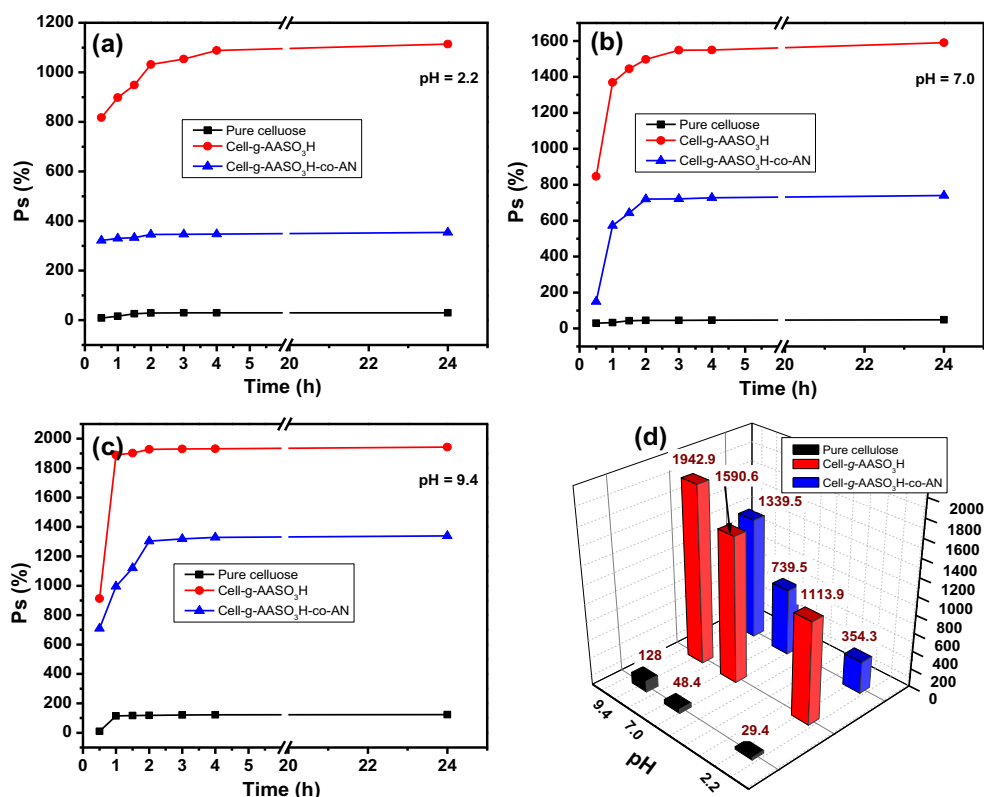
for Cell-g-AASO₃H, and Cell-g-AASO₃H-co-AN, respectively.

Applications of the grafted cellulosic copolymer for dye adsorption

Effect of contact time

Batch experiments were conducted using 50 mL of the 20 ppm dye solutions and 0.05 g of the pure cellulose and grafted copolymers with maximum P_g . The variations of percent dye removal (D_e) was studied with respect to contact time ranging from 10 to 120 min for cationic MG and CV dyes with polymeric samples at 25 °C temperature and at pH 7.0. For all the batch experiments, the D_e values were found to increase with time and the equilibrium was established after about 120 min. For pure cellulose, Cell-g-AASO₃H and Cell-g-AASO₃H-co-AN the initial rapid rates of adsorption of the dyes onto the surface of the copolymers are due to the availability of sufficient active sites on the adsorbent surface initially which gradually decreases with time. Further increase in the contact time practically exhibited no effect on the D_e value of dye molecules. Further, for cationic dyes, the D_e values are much higher for Cell-g-AASO₃H (MG = 95.63%, CV = 98.93%) graft copolymer as compared to bare cellulose (MG = 10.72%, CV = 8.3%) and Cell-g-AASO₃H-co-AN

Fig. 5 Swelling properties of cellulose and its graft copolymers at (a) pH = 2.2, (b) pH = 7.0, (c) pH = 9.4 and (d) Comparative percent swelling cellulose and its graft copolymers after 24 h



(MG = 30.12%, CV = 55.85%) grafted copolymer (Fig. 6a and b). The results are in good agreement with the swelling studies conducted at pH 7.0. This may be also attributed to the incorporation of the negatively charged sulphonic acid ($-SO_3^-$) groups after grafting of the cellulose backbone which can easily attract the cationic dyes such as MG and CV. Due to less swelling behavior of Cell-*g*-AASO₃H-*co*-AN grafted copolymer in contrast to Cell-*g*-AASO₃H, D_e of the former was lower than the latter. In case of cellulose minimum D_e was also recorded as least P_s was observed at pH 7.0 for cellulose. The order of adsorption of cationic dyes by polymeric samples is observed as Cell-*g*-AASO₃H > Cell-*g*-AASO₃H-*co*-AN > Cellulose. Grafting of the AASO₃H monomers onto the cellulose backbone improved swelling and D_e drastically for cationic dyes. It can also be inferred from the results that the hydrophobic nature of AN in Cell-*g*-AASO₃H-*co*-AN lowered the extent of adsorption of cationic dyes as compared to the Cell-*g*-AASO₃H copolymer.

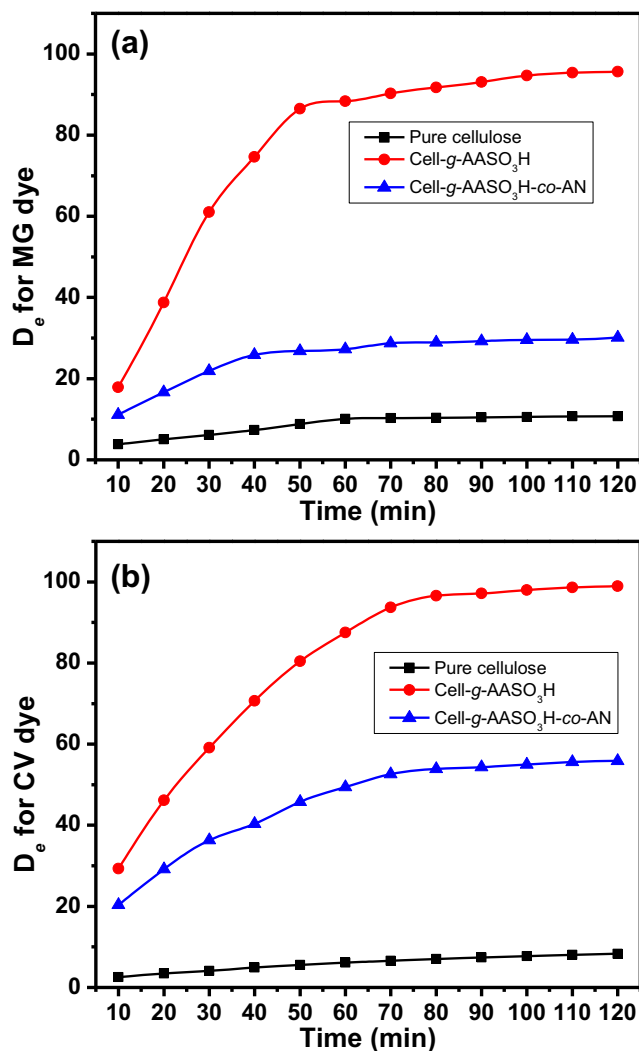


Fig. 6 Percent dye removal as a function of contact time for (a) MG and (b) CV dyes

It is important to mention here is that, the adsorption studies of the grafted copolymers were also evaluated for anionic congo red (CR) dye. However, as compared to cationic dyes, the rate of adsorption for anionic CR dye was quite low, though D_e values were observed to increase with time and the equilibrium was established after 8 h of contact time. Pure cellulose, Cell-*g*-AASO₃H, and Cell-*g*-AASO₃H-*co*-AN copolymers adsorbed 3.33%, 6.046% and 4.85% CR dye after 8 h of contact time at pH 7.0, which is very low as compared to adsorption of cationic dyes. The lower rate of the adsorption for CR dye may be due to the electrostatic repulsions between the anionic dye and negatively charged functional groups on cellulose and its graft copolymers. In contrast, MG and CV dyes have positively charged amine moieties that are strongly attracted towards negatively charged functional groups on cellulose and its graft copolymers. Hence, adsorption data for the anionic CR dye is not discussed in this manuscript.

Effect of temperature

Effect of temperature on dye adsorption batch experiments was studied within the temperature range of 20–40 °C with an interval of 5 °C for optimum contact time evaluated in the earlier step. Maximum D_e for cationic MG and CV dyes was observed for all polymeric samples at 30 °C and 25 °C respectively in a contact time of 2 h (Fig. 7a). The D_e values followed the order Cell-*g*-AASO₃H > Cell-*g*-AASO₃H-*co*-AN > pure cellulose at optimized temperatures.

For MG dye the D_e values for Cell-*g*-AASO₃H, Cell-*g*-AASO₃H-*co*-AN, and pure cellulose were found to be 99.88%, 32.44%, and 11.33%, respectively at 30 °C. Cell-*g*-AASO₃H showed the almost complete removal of for CV dye (99.93%) at 25 °C from 50 mL of the 20 ppm dye solutions. Low adsorption of the dyes at a higher temperature may be attributed to the faster rates of desorption of the dyes molecules as compared to the adsorption.

Effect of pH

Another important external parameter, which affects the chemistry of the functional moieties and hence the D_e of adsorbents, is the pH of the medium. Dye adsorption studies for cellulose and graft copolymers were performed at three pH 2.2, 7.0 and 9.4. For cationic dyes the D_e of pure cellulose was reported to be very low at all the pH values as compared to Cell-*g*-AASO₃H and Cell-*g*-AASO₃H-*co*-AN copolymers. With the rise in pH of the medium from 2.2 to 9.4, the D_e of the pure cellulose towards cationic dyes was marginally increased. For adsorption of MG dye, the graft copolymers of cellulose followed the order 7.0 > 2.2 > 9.4, while for CV dye the observed order was 7.0 > 9.4 > 2.2. Cell-*g*-AASO₃H exhibited maximum D_e of 99.88% and 98.93% for MG and CV

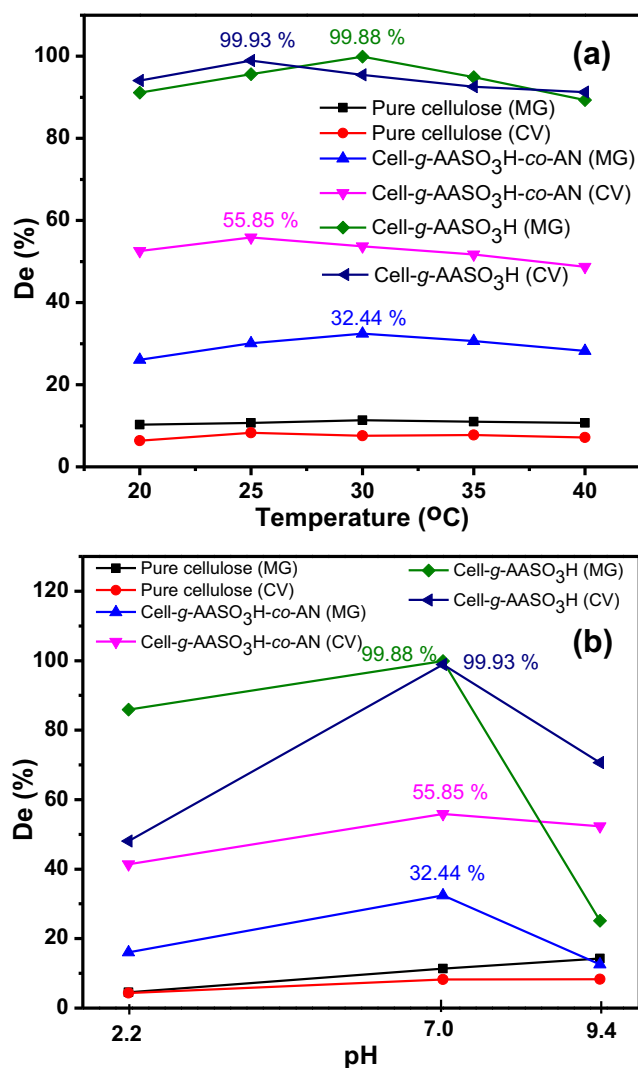


Fig. 7 Percent dye removal of cationic dyes by cellulosic adsorbents (a) as a function of temperature and (b) as a function of pH

dyes, respectively and Cell-g-AASO₃H-co-AN showed maximum D_e of 32.44% and 55.85% for MG and CV dyes, respectively at pH = 7.0 after 2 h of contact time (Fig. 7b).

This behavior can be explained on the basis of protonation-deprotonation of the $-SO_3^-$ groups of Cell-g-AASO₃H and hydrolysis of $-CN$ groups of Cell-g-AASO₃H-co-AN at different pH conditions. Under acidic conditions (pH = 2.2), the protonation of the $-SO_3^-$ groups increases the magnitude of the electrostatic repulsions for the cationic dyes. Under neutral or alkaline pH conditions, deprotonation is resulted favoring reverse trends for cationic dyes. In spite of the higher degree of deprotonation the $-SO_3^-$, $-CONH_2$ and $-COO^-$ groups in alkaline medium with pH 9.4, as compared to neutral pH of 7.0, low extent of adsorption capacity of grafted copolymers for cationic dyes may be attributed to the strong electrostatic attractions between the OH^- ions present in the medium and the cationic sites of the dye molecules blocking the later for the adsorption onto the deprotonated $-SO_3^-$ groups.

Table 4 Kinetics parameters for the adsorption of cationic dyes on graft copolymers

Kinetic models ^a	Cell-g-AASO ₃ H		Cell-g-AASO ₃ H-co-AN	
	MG	CV	MG	CV
Pseudo-first order				
k_1	6.257×10^{-2}	4.463×10^{-2}	3.436×10^{-2}	3.886×10^{-2}
q_e	36.49	28.59	8.2672	12.7282
R^2	0.99145	0.99066	0.99145	0.99168
Pseudo-second order				
k_2	2.91×10^{-3}	1.372×10^{-3}	4.235×10^{-3}	2.851×10^{-3}
q_e	23.031	25.246	7.918	11.803
R^2	0.99887	0.99954	0.99566	0.99598
q_e (exp)	19.98	19.79	6.44	11.17
Elovich model				
α	2.12	1.554	0.5807	1.1635
β	0.1749	0.163	0.5765	0.3241
R^2	0.92438	0.974	0.99715	0.98080
Intra-particle diffusion				
K_{IP}	0.238	0.369	0.525	1.243
C	17.484	15.854	0.938	0.263
R^2	0.88988	0.8547	0.97313	0.99682

^a q_e and q_t = adsorption capacities in $mg \cdot g^{-1}$ at equilibrium and at time t , respectively. k_1 , k_2 = pseudo-first order (min^{-1}) and pseudo-second order rate constant ($g \cdot mg^{-1} \cdot min^{-1}$). α = initial adsorption rate ($mg \cdot g^{-1} \cdot min^{-1}$) β = desorption constant ($g \cdot mg^{-1}$), k_{IP} = Intra-particle diffusion rate constant [$mg/(g \cdot t)^{1/2}$ or $m \cdot mol/(g \cdot t)^{1/2}$], C = Constant parameter corresponding to boundary layer thickness ($mg \cdot g^{-1}$)

Kinetics studies for dye adsorption applications

The kinetic behavior of Cell-g-AASO₃H and Cell-g-AASO₃H-co-AN towards the adsorption of different dyes was evaluated using pseudo-first-order, pseudo-second order, Elovich's kinetic and Intra-particle diffusion models (Fig. S1 and Fig. S2). The equation along with different parameters, their meanings and units are reported elsewhere in the literature [56, 57]. The various adsorption parameters like rate constants, adsorption capacities (q_e) and correlation regression coefficients (R^2) calculated from these kinetics model plots are given in Table 4. The adsorption measurements were carried out at optimized temperatures and pH values using 50 mL of 20 ppm dye solutions, accurately weighed adsorbent dose of 0.05 g and contact time of 0–120 min for cationic dyes. The pseudo-first-order rate constants (k_1) were higher for Cell-g-AASO₃H as compared to a Cell-g-AASO₃H-co-AN copolymer for all the model dyes. However, for both the cationic dyes, the pseudo-second-order model seems to be best-fitted with the experimental data as compared to other models. This confirms the fact that the rate-determining step for the dye adsorption involves physicochemical interactions between the dye molecules and the adsorbent. The view is further

supported by the higher values of correlation regression coefficients (R^2) for pseudo-second-order kinetics models as compared to pseudo-first order and Elovich's kinetics models. Further, the q_e values calculated from the pseudo-second-order model for both the cationic dyes are closer to the experimental q_{exp} values as compared to pseudo-first order kinetics models (Table 4).

Thus, the initial physical interaction between the dye molecules and the copolymer chains are followed by strong physicochemical interactions in case of for Cell-*g*-AASO₃H copolymer. For MG and CV higher values of α as compared to β values in Elovich's kinetic confirm the higher rate of the adsorption of the dyes than desorption. The regression coefficient constants were 0.92438 and 0.9740 for MG and CV dyes, respectively which further reflect the applicability of the Elovich's kinetic model for Cell-*g*-AASO₃H and Cell-*g*-AASO₃H-*co*-AN copolymers (Table 4). A larger value of boundary layer thickness parameter (C) for Cell-*g*-AASO₃H as compared to a Cell-*g*-AASO₃H-*co*-AN copolymer for MG and CV dyes in intra-particle diffusion model revealed a greater boundary layer diffusion effect for the former. Such type of dye adsorption behavior has also been reported earlier [58].

Adsorption isotherms models for dye adsorption applications

Freundlich, Langmuir and Temkin isotherms were studied for the adsorption of cationic dyes from the 50 mL aqueous solutions with concentrations ranging from 5.0–70 ppm at an optimized contact time, temperature and pH conditions (Fig. S3 and Fig. S4). The linear forms for these adsorption models along with the meaning and units of different parameters are reported elsewhere in the literature [56, 57, 59]. Adsorption parameters, constants and linear correlation coefficients (R^2) obtained from different adsorption isotherms for various dyes are listed in Table 5. For all the dyes the values of $\frac{1}{n}$ are between $0 \rightarrow 1$ which indicate a favorable physisorption of the dyes onto the surface of the copolymers [60]. The data also support the poor adsorption behavior of the Cell-*g*-AASO₃H-*co*-AN copolymer than Cell-*g*-AASO₃H copolymer. Greater R^2 values for Langmuir adsorption isotherm, as compared to the Freundlich adsorption isotherm confirm the better suitability of the former for explaining the adsorption of the dye molecules onto grafted copolymers. The maximum adsorption capacity, q_m obtained from the Langmuir adsorption isotherm are 61.46 and 55.71 mg.g⁻¹ for Cell-*g*-AASO₃H and 44.09 and 54.71 mg.g⁻¹ for Cell-*g*-AASO₃H-*co*-AN copolymer against MG and CV, dyes, respectively.

For all the dye concentrations, the values of the dimensionless quantity, R_L ranged between $0 \rightarrow 1$ which further supports the better fitting of the adsorption data into Langmuir adsorption isotherm model as compared to Freundlich

adsorption isotherm model (Table 5). A higher value of Temkin isotherm equilibrium binding constant (A_T) for CV dye as compared to MG dye suggests a better preference of the Cell-*g*-AASO₃H copolymer for CV dye than MG. Very low values of A_T for Cell-*g*-AASO₃H-*co*-AN copolymer as compared to Cell-*g*-AASO₃H copolymer against all the two model dyes confirm its poor adsorption capacities (Table 5). However, the regression correlation coefficient values for both the dyes obtained from the Temkin adsorption isotherm model were found to be less as compared to the Langmuir adsorption isotherms.

The results for the different adsorption isotherm models confirm that for cationic dyes, the adsorption was monolayered and took place at certain specific, energetically identical and homogeneous sites i.e. appended $-SO_3^-$ groups on the surface of the Cell-*g*-AASO₃H copolymer and $-SO_3^-$ and $-CONH_2$ groups (generated by hydrolysis of $-CN$ groups of AN comonomers) in Cell-*g*-AASO₃H-*co*-AN copolymer. The adsorption results, in terms of ease of synthesis of adsorbent and other adsorption parameters for Cell-*g*-AASO₃H graft copolymer for cationic dyes are better as compared to the other adsorbent materials reported in literature (Table 6).

Applications of the grafted cellulosic copolymer for metal ion sorption

Effect of contact time

Sorption behavior of 0.05 g pure cellulose, Cell-*g*-AASO₃H and Cell-*g*-AASO₃H-*co*-AN copolymers for Pb(II) ions with 100 ppm concentration at 7.0 pH, and 25 °C temperature was studied as a function of contact time (Fig. 8a). All the samples showed significant sorption of Pb(II) ions up to 120 min, but after that, no significant sorption was recorded. Thus, after a contact time of 120 min, the sorption sites of the sorbents were saturated. Further, both the grafted copolymers exhibited remarkably improved sorption behavior as compared to pure cellulose. Deprotonation of the sulfonic acid groups of the AASO₃H groups in Cell-*g*-AASO₃H copolymer into the $-SO_3^-$ groups provides the favorable active sites for the sorption of positively charged Pb(II) ions. Introduction of AN as binary comonomer in Cell-*g*-AASO₃H-*co*-AN, further provides $-CN$ groups as active sites for better sorption of Pb(II) ions as compared to Cell-*g*-AASO₃H though marginal. Very small increase in metal ion sorption capacity of Cell-*g*-AASO₃H-*co*-AN as compared to Cell-*g*-AASO₃H, may be attributed to the hydrophobic nature of the AN comonomer which results in a slight increase in percent grafting (Table 2). For pure cellulose, Cell-*g*-AASO₃H and Cell-*g*-AASO₃H-*co*-AN copolymers P_g of 13.5, 41.8 and 43.3% were observed, respectively for Pb(II) ions.

Table 5 Adsorption parameters for the adsorption of cationic dyes on graft copolymers

Adsorption isotherm models ^a	Cell-g-AASO ₃ H		Cell-g-AASO ₃ H-co-AN	
	MG	CV	MG	CV
Freundlich isotherm				
K _F	26.83	26.46	18.33	21.58
1/n	0.396	0.315	0.285	0.399
R ²	0.97302	0.96332	0.96241	0.91474
Langmuir isotherm				
K _L	1.277	1.561	0.797	1.097
q _m	61.46	55.71	44.09	54.71
R ²	0.99153	0.99365	0.99102	0.99677
Temkin isotherm				
A _T	43.73	135.39	1.052	1.104
b _T	274.33	373.92	467.28	287.86
RT/b _T	9.03	6.74	5.30	8.75
R ²	0.96366	0.92377	0.94837	0.98672

^a q_e = Amount of dye adsorbed on the adsorbent at equilibrium ($\text{mg}\cdot\text{g}^{-1}$), K_F = Freundlich adsorption isotherm constant, n = Heterogeneity factor that defines the adsorption intensity of the adsorbent, C_o , C_e = Initial and equilibrium metal ion concentrations, respectively in $\text{mg}\cdot\text{L}^{-1}$, q_m = Monolayer saturation adsorption ($\text{mg}\cdot\text{g}^{-1}$), K_L = Langmuir adsorption isotherm constant related to the adsorption energy, R = Gas constant, T = Absolute temperature (K), A_T = Temkin isotherm equilibrium binding constant ($\text{mL}\cdot\text{mg}^{-1}$), b_T = Temkin constant interaction parameter)

Effect of temperature

Pb(II) metal ion sorption efficiencies of pure cellulose and grafted copolymers were evaluated as a function of temperature ranging from 20 to 40 °C at pH 7.0, 100 ppm concentration of Pb(II), and contact time of 120 min (Fig. 8b). With the initial increase in temperature, the sorption capacities for

Pb(II) ions were increased for all the samples up to 30 °C. The increased swelling, weakening of intermolecular polymer-polymer interactions leading to exposure of the active sites, and faster diffusion of the metal ions into the polymer matrix with an increase in temperature improved the metal ions sorption capacities and P_u of the polymeric samples [16]. Further, increased temperature also provides the required

Table 6 The optimized adsorption parameters reported for adsorption of MG and CV dyes onto different adsorbents

Adsorbent	Dose (g/L)	Conc. (ppm)	Contact time (min)	pH	Temp. (°C)	De (%)	q _{max} (mg/g)	Ref.
<i>Malachite green dye</i>								
Cell-g-AASO ₃ H-co-GMA	1.0	20	80	7	30	100	46.23	[14]
Cell-g-AASO ₃ H-co-AAc	1.0	20	120	7	30	48.33	4.42	[16]
Av-cl-poly(AA-ipn-AAm)	5.0	10	180	4.5	25	97.30	–	[61]
β- Cyclodextrins- Carboxymethylcellulose	1.5	40	120	8	25	–	8.2	[62]
Aloe vera-poly(acrylic acid-co-acrylamide)	5.0	25	180	4.5	RT	94.30	–	[63]
Chitosan beads 1-butyl-3-methylimidazolium acetate	0.4	10	20	4	RT	~50.0	~40	[64]
Aca-NaAlg-cl-poly(AA)	5.0	25	20 h	9	35	95.39	–	[65]
Carbonized pomegranate Peel	2.0	40	90	6	50	99.10	19.82	[66]
Cell-g-AASO ₃ H	1.0	20	120	7	30	99.88	61.46	<i>This work</i>
Cell-g-AASO ₃ H-co-AN	1.0	20	120	7	30	32.43	44.09	<i>This work</i>
<i>Crystal violet dye</i>								
Cell-g-AASO ₃ H-co-GMA	1.0	20	80	7	30	100	53.53	[14]
Cell-g-AASO ₃ H-co-AAc	1.0	20	120	7	25	50.17	9.57	[16]
Chitin nanowhiskers	50.0	250	–	–	RT	79.13	39.56	[67]
Aca-NaAlg-cl-poly(AA)	5.0	25	20 h	9	35	96.56	–	[65]
Xan-aca-cl-poly(AAm)	5.0	10	16 h	9	20	95.42	–	[68]
Functionalized cellulosic microfibers	0.2	200	60	7	25	~100	~856	[69]
Coniferous pinus bark powder	1.0	20	120	8	30	99.50	–	[70]
Cell-g-AASO ₃ H	1.0	20	120	7	25	98.93	55.71	<i>This work</i>
Cell-g-AASO ₃ H-co-AN	1.0	20	120	7	25	55.85	54.71	<i>This work</i>

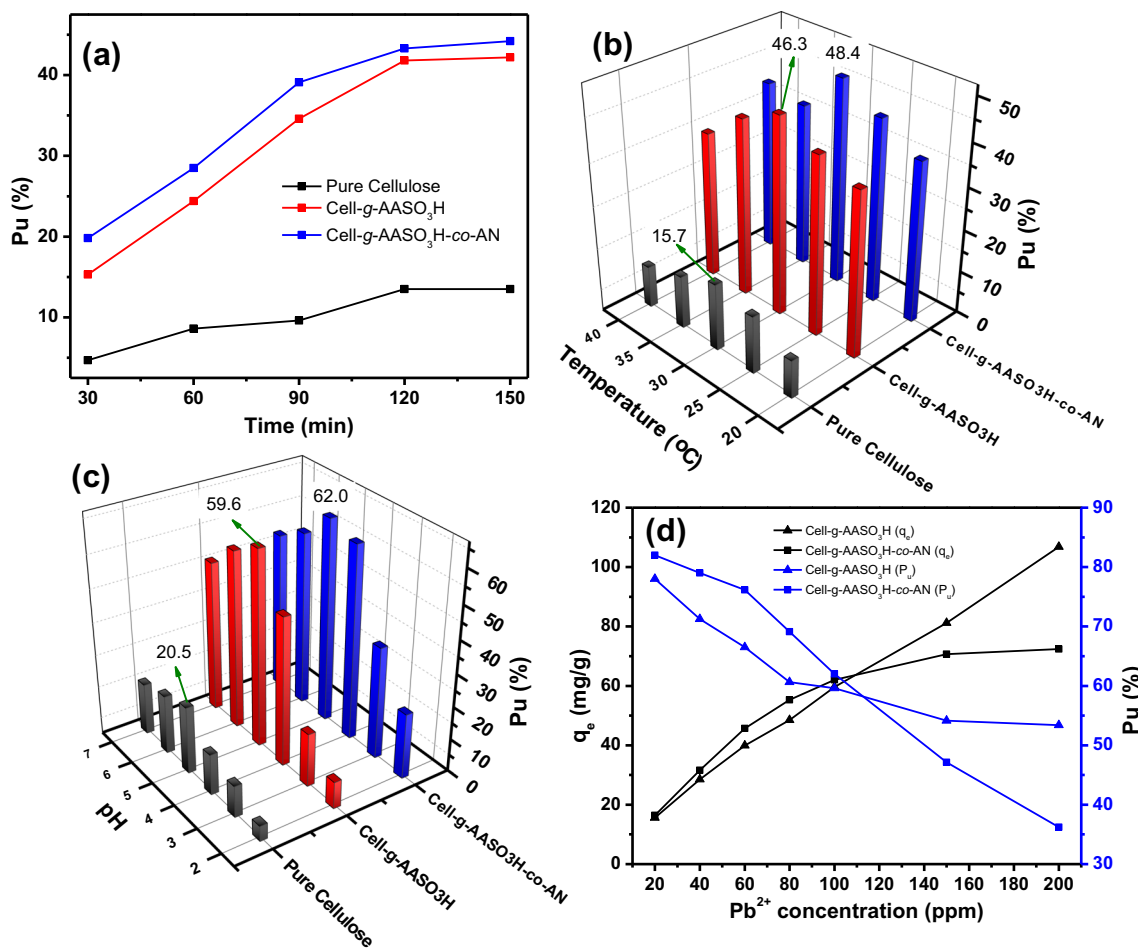


Fig. 8 Pb(II) metal ion uptake capacities of Cell-g-AASO₃H and Cell-g-AASO₃H-co-AN copolymers as a function of (a) Contact time, (b) Temperature, (c) pH and (d) initial Pb(II) ion concentrations

activation energy for the chemisorption of the metal ions onto the surface of the copolymers. With a further rise in temperature, the desorption rates which lowered the P_u capacities for pure cellulose and grafted copolymers. At an optimized temperature of 30 °C for pure cellulose, Cell-g-AASO₃H and Cell-g-AASO₃H-co-AN copolymers observed P_u values were 15.7, 46.3 and 48.4%, respectively.

Effect of pH

The protonation-deprotonation equilibrium of the $-SO_3^-$ groups of Cell-g-AASO₃H and hydrolysis $-CN$ groups of Cell-g-AASO₃H-co-AN at different pH conditions, significantly affect the Pb(II) metal ions sorptions by the grafted copolymers. Deprotonation of the $-SO_3^-$ with increased pH fabricates the $-SO_3^-$ groups which strongly attracts the positively charged Pb(II) metal ions. The uptake studies of the Pb(II) ions by pure cellulose and grafted copolymers were studied in the pH range of 2.0–7.0 with the initial concentrations of 100 ppm at optimized conditions of temperature and

contact time. For all the sorbent samples maximum metal ions uptake was reported at pH 5.0 (Fig. 8c). Below and above this optimized pH, metal ions uptake capacities were low which is in good agreement with the surface complexation theory, according to which at low pH conditions, metal ions and H⁺ ions of the medium compete for the negatively charged active sites of the sorbent material [14, 71]. Precipitation of the metal ions beyond pH 7.0, lowers the metal ion uptake capacities of the grafted copolymers.

Effect of metal ion concentration

Under optimum conditions of contact time, temperature, and pH, the sorption behavior of Cell-g-AASO₃H and Cell-g-AASO₃H-co-AN copolymers was evaluated for different concentrations of Pb(II) metal ions ranging from 10 to 200 ppm. Figure 8d represents the variations of the equilibrium sorption amount ‘ q_e ’, percent uptake (P_u) for Cell-g-AASO₃H and Cell-g-AASO₃H-co-AN copolymers. For Cell-g-AASO₃H-co-AN copolymers, P_u values were higher

Table 7 Kinetics parameters for sorption of Pb(II) ions by cellulose and its graft copolymers

Kinetic models	Pure cellulose	Cell-g-AASO ₃ H	Cell-g-AASO ₃ H-co-AN
Pseudo-first order			
k_1	2.47×10^{-3}	3.934×10^{-2}	3.932×10^{-2}
q_e	77.11	194.57	186.22
R^2	0.99122	0.80837	0.83236
Pseudo-second order			
k_2	1.47×10^{-4}	2.31×10^{-5}	4.44×10^{-5}
q_e	46.08	178.89	142.86
R^2	0.99548	0.99805	0.99861
Elovich model			
α	0.691	1.807	2.036
β	0.108	0.035	0.036
R^2	0.99471	0.97843	0.98598
Intra-particle diffusion			
K_{IP}	2.35	7.25	7.13
C	5.019	20.16	16.046
R^2	0.99646	0.99937	0.99993

than Cell-g-AASO₃H copolymer for low concentrations (20–100 ppm), but for higher Pb(II) concentrations (150 and 200 ppm) P_u values were higher for Cell-g-AASO₃H than Cell-g-AASO₃H-co-AN copolymer. The q_e values followed opposite trends as compared to P_u values for the Cell-g-AASO₃H and Cell-g-AASO₃H-co-AN.

Kinetics studies for metal ion sorption applications

Similar to dyes, various kinetic models viz. pseudo first order, pseudo-second order, Elovich's and intraparticle diffusion kinetic models were applied to the sorption data obtained for the sorption of Pb(II) using Cell-g-AASO₃H and Cell-g-AASO₃H-co-AN copolymers (Fig. S5). From

coefficient of determinant (R^2), the pseudo-second-order kinetic models were best fitted for Cell-g-AASO₃H and Cell-g-AASO₃H-co-AN copolymers. This indicates that the chemisorption is the controlling force for the sorption of Pb(II) ions. The highly fitted plot, as obtained for Elovich kinetic model, suggests that the binding mechanisms such as ion exchange, chelation, and ion entrapment etc. control the sorption of Pb(II) ions onto Cell-g-AASO₃H and Cell-g-AASO₃H-co-AN copolymers [72]. Further, significantly higher values of initial adsorption rate ' α ' as compared to desorption constant ' β ' indicate that adsorption is more favorable than desorption for Pb(II) ions onto Cell-g-AASO₃H and Cell-g-AASO₃H-co-AN copolymers (Table 7). Comparable values of boundary layer

Table 8 Adsorption isotherm parameters for sorption of Pb(II) ions by Cell-g-AASO₃H and Cell-g-AASO₃H-co-AN copolymers

Adsorption isotherm models	Pure cellulose	Cell-g-AASO ₃ H	Cell-g-AASO ₃ H-co-AN
Freundlich isotherm			
K_F	1.11	6.253	12.864
$1/n$	0.167	0.6125	0.4008
R^2	0.97982	0.99551	0.85479
Langmuir isotherm			
K_L	0.129	0.018	0.084
q_m	23.54	154.32	181.49
R^2	0.99508	0.86552	0.9988
Temkin isotherm			
A_T	1.502	0.6601	0.9939
b_T	84.71	89.75	154.58
RT/b_T	2.974	28.068	16.30
R^2	0.98455	0.87061	0.95845

Table 9 The adsorption parameters reported for different sorbents for the sorption of Pb(II) onto different sorbents

Adsorbent	Dose (g/L)	Conc. (ppm)	Contact time (h)	pH	T (°C)	q _{max} (mg/g)	Ref.
Cell-g-NIPAM-co-GMA	1.0	20–200	6.0	5.0	30	119.76	[13]
Cellulose xanthate	4.0	50–1000	0.5	5.5	30	131.41	[74]
Biochar	–	0–1000	0.5	5.8	30	37.40	[75]
Magnetic biochar						44.62	
Hydroxylated biochar						146.8	
<i>Cinnamomum camphora</i> biochar	4.0	50–1000	0.5	5.8	30	98.33	[76]
Sugar cane biochar	1.0	–	–	5.0	25	86.96	[77]
Orange peel biochar						27.86	
Cell-poly(glycidyl methacrylate)	–	250	–	5.0	RT	52.00	[36]
Hemicell-AASO ₃ H-AAc	2.0	100	1.0	5.0	25	48.30	[78]
Hemicell-AASO ₃ H-APA						65.80	
Hemicell-AASO ₃ H-AAm						40.80	
Cellulose fibre /poly(NIPAM-co-AAc)	1.0	324	3.0	6.0	20	80.8	[79]
Cell-g-AASO ₃ H	1.0	20–200	6.0	5.0	30	154.32	<i>This work</i>
Cell-g-AASO ₃ H-co-AN	1.0	20–200	6.0	5.0	30	181.49	<i>This work</i>

parameter (C) calculated from intraparticle diffusion kinetic model for sorption of Pb(II) ions indicate that the boundary layer effects are controlling the diffusion rate of metal ions through the surface of the grafted copolymer [73].

Adsorption isotherms for metal ion sorption applications

The sorption capacities of the Cell-g-AASO₃H and Cell-g-AASO₃H-co-AN copolymers were studied for different Pb(II) ion concentrations ranging from 20 to 200 ppm at the optimized conditions and the data obtained were used to explore sorption parameters for different adsorption isotherm models similar to the dye adsorption applications (Fig. S6). From the value of the determinant coefficient, Freundlich and Langmuir adsorption isotherm plots were found to best fitted for Cell-g-AASO₃H and Cell-g-AASO₃H-co-AN copolymers, respectively for the sorption of Pb(II) ions (Table 8). This indicates that for Cell-g-AASO₃H-co-AN copolymer, monolayered sorption of the Pb(II) ions occurs onto the active sites [74]. However, values of dimensionless quantity R_L for different concentrations ranging from 0 → 1 for both the copolymers which support the monolayered sorption of the metal ions. Maximum adsorption capacities for Cell-g-AASO₃H and Cell-g-AASO₃H-co-AN copolymers observed from Langmuir adsorption isotherm were 154.32 and 79.94 mg.g⁻¹ respectively. Comparative higher R^2 values for Cell-g-AASO₃H-co-AN as compared to Cell-g-AASO₃H copolymer suggest a more uniform distribution of the binding energies for Cell-g-AASO₃H-co-AN as compared to Cell-g-AASO₃H copolymer during adsorption. The comparative analysis of the sorption efficiencies of Cell-g-AASO₃H and Cell-g-AASO₃H-co-AN copolymers with those of the already reported

copolymers/sorbents shows that as-synthesized copolymers are excellent sorbents for Pb(II) metal ions (Table 9).

Conclusion

Cellulose-based biosorbents were synthesized from agricultural residue, rice husk. At optimized conditions i.e. [AASO₃H] = 96.501×10^{-2} mol L⁻¹, initiator; [KPS] = 18.5×10^{-2} mol L⁻¹, cross-linker; [N,N'-MBA] = 0.1 g (5 wt% of monomer AASO₃H), temperature = 60 °C and time = 5 min in 10 mL of water as solvent, maximum P_g of 249.0 was observed for Cell-g-AASO₃H. For Cell-g-AASO₃H-co-AN binary copolymer, maximum P_g of 267.0 was recorded at 2.5 M ratio of AN *w.r.t.* AASO₃H concentration. Dye adsorption behavior studied for cationic dyes followed the order Cell-g-AASO₃H > Cell-g-AASO₃H-co-AN > cellulose, whereas, for Pb(II) metal ions, percent uptake by Cell-g-AASO₃H-co-AN (62.0%) was slightly higher than Cell-g-AASO₃H (59.6%) at optimized conditions of contact time, temperature and pH. Almost complete adsorption was reported for MG and CV dyes at pH 7.0 and contact time 2 h from 50 mL of 20 ppm dye solutions. For dye adsorption study, the pseudo-second-order model seems to be best-fitted with the experimental data as compared to pseudo-first order and Elovich's kinetics models. The maximum adsorption capacity, obtained from the Langmuir adsorption isotherm for MG and CV dyes were 61.46 and 55.71 mg.g⁻¹ respectively, for Cell-g-AASO₃H. For Pb(II) ions maximum adsorption capacities from Langmuir adsorption isotherm were 154.32 and 181.49 mg.g⁻¹ for Cell-g-AASO₃H and Cell-g-AASO₃H-co-AN, respectively.

Acknowledgments Authors are thankful to Department of Science & Technology (DST), Ministry of Science & Technology, New Delhi for providing instrumentation facility under DST-FIST scheme to DAV College, Jalandhar. One of the authors, Rajesh Kumar, acknowledges I.K Gujral Punjab Technical University, Kapurthala, Punjab for providing research support to him. Dr. Rajeev Kr. Sharma acknowledges UGC, New Delhi for sanctioning MRP no. F.8-4(92)/2015 (MRP/NRCB).

References

- Carneiro PA, Umbuzeiro GA, Oliveira DP, Zanoni MVB (2010) Assessment of water contamination caused by a mutagenic textile effluent/dyehouse effluent bearing disperse dyes. *J Hazard Mater* 174:694–699. <https://doi.org/10.1016/j.jhazmat.2009.09.106>
- Tsuboy MS, Angeli JPF, Mantovani MS, Knasmüller S, Umbuzeiro GA, Ribeiro LR (2007) Genotoxic, mutagenic and cytotoxic effects of the commercial dye CI disperse blue 291 in the human hepatic cell line HepG2. *Toxicol in Vitro* 21:1650–1655. <https://doi.org/10.1016/j.tiv.2007.06.020>
- Bharathi KS, Ramesh ST (2013) Removal of dyes using agricultural waste as low-cost adsorbents: a review. *Appl Water Sci* 3:773–790. <https://doi.org/10.1007/s13201-013-0117-y>
- Okieimen FE, Sogbaike CE, Ebhoaye JE (2005) Removal of cadmium and copper ions from aqueous solution with cellulose graft copolymers. *Sep Purif Technol* 44:85–89. <https://doi.org/10.1016/j.seppur.2004.11.003>
- Badiei M, Asim N, Jahim JM, Sopian K (2014) Comparison of chemical pretreatment methods for cellulosic biomass. *APCBEE Proc* 9:170–174. <https://doi.org/10.1016/j.apcbee.2014.01.030>
- Akhtar N, Gupta K, Goyal D, Goyal A (2016) Recent advances in pretreatment technologies for efficient hydrolysis of lignocellulosic biomass. *Environ Prog Sustain Energy* 35:489–511. <https://doi.org/10.1002/ep.12257>
- Chauhan GS, Dhiman SK, Guleria LK, Kaur I (2002) Polymers from renewable resources: kinetics studies of the radiochemical graft copolymerization of styrene onto cellulose extracted from pine needles and the effect of some additives on the grafting parameters in an aqueous medium. *J Appl Polym Sci* 83:1490–1500. <https://doi.org/10.1002/app.10142>
- Chauhan GS, Lal H, Mahajan S (2004) Synthesis, characterization, and swelling responses of poly(N-isopropylacrylamide)- and hydroxypropyl cellulose-based environmentally sensitive biphasic hydrogels. *J Appl Polym Sci* 91:479–488. <https://doi.org/10.1002/app.13135>
- Hokkanen S, Bhatnagar A, Sillanpa M (2016) A review on modification methods to cellulose-based adsorbents to improve adsorption capacity. *Water Res* 91:156–173. <https://doi.org/10.1016/j.watres.2016.01.008>
- Sahoo PK, Jena DK (2018) Synthesis and study of mechanical and fire retardant properties of (carboxymethyl cellulose -g-polyacrylonitrile)/montmorillonite biodegradable nanocomposite. *J Polym Res* 25:260. <https://doi.org/10.1007/s10965-018-1659-3>
- Kang H, Liu R, Huang Y (2015) Graft modification of cellulose: methods, properties and applications. *Polym (United Kingdom)* 70:A1–A16. <https://doi.org/10.1016/j.polymer.2015.05.041>
- Chauhan GS, Guleria L, Sharma R (2005) Synthesis, characterization and metal ion sorption studies of graft copolymers of cellulose with glycidyl methacrylate and some comonomers. *Cellulose* 12:97–110. <https://doi.org/10.1023/B:CELL.0000049349.66326.5e>
- Kumar R, Sharma RK, Singh AP (2019) Grafting of cellulose with N-isopropylacrylamide and glycidyl methacrylate for efficient removal of Ni(II), Cu(II) and Pd(II) ions from aqueous solution. *Sep Purif Technol* 219:249–259. <https://doi.org/10.1016/j.seppur.2019.03.035>
- Sharma RK, Kumar R, Singh AP (2019) Metal ions and organic dyes sorption applications of cellulose grafted with binary vinyl monomers. *Sep Purif Technol* 209:684–697. <https://doi.org/10.1016/j.seppur.2018.09.011>
- Goel NK, Kumar V, Misra N, Varshney L (2015) Cellulose based cationic adsorbent fabricated via radiation grafting process for treatment of dyes waste water. *Carbohydr Polym* 132:444–451. <https://doi.org/10.1016/j.carbpol.2015.06.054>
- Kumar R, Sharma RK, Singh AP (2018) Removal of organic dyes and metal ions by cross-linked graft copolymers of cellulose obtained from the agricultural residue. *J Environ Chem Eng* 6:6037–6048. <https://doi.org/10.1016/j.jece.2018.09.021>
- Bello K, Sarojini BK, Narayana B (2019) Design and fabrication of environmentally benign cellulose based hydrogel matrix for selective adsorption of toxic dyes from industrial effluvia. *J Polym Res* 26:62. <https://doi.org/10.1007/s10965-019-1724-6>
- Zhao J, Lu C, He X, Zhang X, Zhang W, Zhang X (2015) Polyethylenimine-grafted cellulose nanofibril aerogels as versatile vehicles for drug delivery. *ACS Appl Mater Interfaces* 7:2607–2615. <https://doi.org/10.1021/am507601m>
- Du H, Han R, Tang E et al (2018) Synthesis of pH-responsive cellulose-g-P4VP by atom transfer radical polymerization in ionic liquid, loading, and controlled release of aspirin. *J Polym Res* 25:205. <https://doi.org/10.1007/s10965-018-1601-8>
- Sharma RK, Singh J, Chauhan GS (2010) Study of immobilization of protease and sorption of bsa on cellulose, cellulose derivatives, and graft copolymers. *BioResources* 5:2547–2555
- Wu Y, Luo X, Li W, Song R, Li J, Li Y, Li B, Liu S (2016) Green and biodegradable composite films with novel antimicrobial performance based on cellulose. *Food Chem* 197:250–256. <https://doi.org/10.1016/j.foodchem.2015.10.127>
- Kale RD, Gorade VG (2018) Preparation of acylated microcrystalline cellulose using olive oil and its reinforcing effect on poly(lactic acid) films for packaging application. *J Polym Res* 25:81. <https://doi.org/10.1007/s10965-018-1470-1>
- Chiappone A, Nair J, Gerbaldi C, Zeno E, Bongiovanni R (2014) Flexible and high performing polymer electrolytes obtained by UV-induced polymer–cellulose grafting. *RSC Adv* 4:40873–40881. <https://doi.org/10.1039/C4RA07299E>
- Masoumi A, Hemmati K, Ghaemy M (2016) Low-cost nanoparticles sorbent from modified rice husk and a copolymer for efficient removal of Pb(II) and crystal violet from water. *Chemosphere* 146:253–262. <https://doi.org/10.1016/j.chemosphere.2015.12.017>
- Chakraborty S, Chowdhury S, Das Saha P (2011) Adsorption of crystal violet from aqueous solution onto NaOH-modified rice husk. *Carbohydr Polym* 86:1533–1541. <https://doi.org/10.1016/j.carbpol.2011.06.058>
- Chowdhury S, Mishra R, Saha P, Kushwaha P (2011) Adsorption thermodynamics, kinetics and isosteric heat of adsorption of malachite green onto chemically modified rice husk. *Desalination* 265:159–168. <https://doi.org/10.1016/j.desal.2010.07.047>
- Zhou Y, Zhang M, Wang X, Huang Q, Min Y, Ma T, Niu J (2014) Removal of crystal violet by a novel cellulose-based adsorbent: comparison with native cellulose. *Ind Eng Chem Res* 53:5498–5506. <https://doi.org/10.1021/ie404135y>
- Zhou Y, Min Y, Qiao H, Huang Q, Wang E, Ma T (2015) Improved removal of malachite green from aqueous solution using chemically modified cellulose by anhydride. *Int J Biol Macromol* 74:271–277. <https://doi.org/10.1016/j.ijbiomac.2014.12.020>
- Zheng X, Li X, Li J, Wang L, Jin W, Liu J, Pei Y, Tang K (2018) Efficient removal of anionic dye (Congo red) by dialdehyde microfibrillated cellulose/chitosan composite film with significantly improved stability in dye solution. *Int J Biol Macromol* 107:283–289. <https://doi.org/10.1016/j.ijbiomac.2017.08.169>
- Ruan C-Q, Strømme M, Lindh J (2018) Preparation of porous 2,3-dialdehyde cellulose beads crosslinked with chitosan and their

- application in adsorption of Congo red dye. *Carbohydr Polym* 181: 200–207. <https://doi.org/10.1016/j.carbpol.2017.10.072>
31. Wang Y, Zhao L, Peng H, Wu J, Liu Z, Guo X (2016) Removal of anionic dyes from aqueous solutions by cellulose-based adsorbents: equilibrium, kinetics, and thermodynamics. *J Chem Eng Data* 61: 3266–3276. <https://doi.org/10.1021/acs.jced.6b00340>
 32. Qiao H, Zhou Y, Yu F, Wang E, Min Y, Huang Q, Pang L, Ma T (2015) Effective removal of cationic dyes using carboxylate-functionalized cellulose nanocrystals. *Chemosphere* 141:297–303. <https://doi.org/10.1016/j.chemosphere.2015.07.078>
 33. Chauhan GS, Chauhan K, Chauhan S, Kumar S, Kumari A (2007) Functionalization of pine needles by carboxymethylation and network formation for use as supports in the adsorption of Cr⁶⁺. *Carbohydr Polym* 70:415–421. <https://doi.org/10.1016/j.carbpol.2007.04.020>
 34. Chauhan GS, Chauhan S, Kumar S, Kumari A (2008) A study in the adsorption of Fe(2+) and NO(3)(-) on pine needles based hydrogels. *Bioresour Technol* 99:6464–6470. <https://doi.org/10.1016/j.biortech.2007.11.044>
 35. Chauhan GS, Mahajan S (2002) Use of novel hydrogels based on modified celluloses and methacrylamide for separation of metal ions from water systems. *J Appl Polym Sci* 86:667–671. <https://doi.org/10.1002/App.10943>
 36. Barsbay M, Kavaklı PA, Tilki S, Kavaklı C, Güven O (2018) Porous cellulosic adsorbent for the removal of Cd (II), Pb(II) and Cu(II) ions from aqueous media. *Radiat Phys Chem* 142:70–76. <https://doi.org/10.1016/j.radphyschem.2017.03.037>
 37. Sokker HH, Gad YH, Ismail SA (2012) Synthesis of bifunctional cellulosic adsorbent by radiation induced graft polymerization of glycidyl methacrylate-co-methacrylic acids. *J Appl Polym Sci* 126: E54–E62. <https://doi.org/10.1002/app.34220>
 38. Monier M, Akl MA, Ali WM (2014) Modification and characterization of cellulose cotton fibers for fast extraction of some precious metal ions. *Int J Biol Macromol* 66:125–134. <https://doi.org/10.1016/j.ijbiomac.2014.01.068>
 39. Sharma RK, Chauhan GS (2009) Synthesis and characterization of graft copolymers of 2-hydroxyethyl methacrylate and some comonomers onto extracted cellulose for use in separation technologies. *BioResources* 4:986–1005
 40. Hajeeth T, Vijayalakshmi K, Gomathi T, Sudha PN (2013) Removal of Cu(II) and Ni(II) using cellulose extracted from sisal fiber and cellulose-g-acrylic acid copolymer. *Int J Biol Macromol* 62:59–65. <https://doi.org/10.1016/j.ijbiomac.2013.08.029>
 41. Hajeeth T, Sudha PN, Vijayalakshmi K, Gomathi T (2014) Sorption studies on Cr (VI) removal from aqueous solution using cellulose grafted with acrylonitrile monomer. *Int J Biol Macromol* 66:295–301. <https://doi.org/10.1016/j.ijbiomac.2014.02.027>
 42. Güçlü G, Gürdağ G, Özgümüş S (2003) Competitive removal of heavy metal ions by cellulose graft copolymers. *J Appl Polym Sci* 90:2034–2039. <https://doi.org/10.1002/app.12728>
 43. Ding Z, Yu R, Hu X, Chen Y, Zhang Y (2014) Graft copolymerization of epichlorohydrin and ethylenediamine onto cellulose derived from agricultural by-products for adsorption of Pb(II) in aqueous solution. *Cellulose*. 21:1459–1469. <https://doi.org/10.1007/s10570-014-0246-y>
 44. Sharma RK, Kumar R, Singh AP (2018) Extraction of cellulose micro-whiskers from rice husk: a greener approach. *J Nanosci Nanotechnol* 18:3702–3708
 45. Sharma RK, Lalita SAP, Chauhan GS (2014) Grafting of GMA and some comonomers onto chitosan for controlled release of diclofenac sodium. *Int J Biol Macromol* 64:368–376. <https://doi.org/10.1016/j.ijbiomac.2013.12.028>
 46. Lalita SAP, Sharma RK (2017) Synthesis and characterization of graft copolymers of chitosan with {NIPAM} and binary monomers for removal of Cr(VI), Cu(II) and Fe(II) metal ions from aqueous solutions. *Int J Biol Macromol* 99:409–426. <https://doi.org/10.1016/j.ijbiomac.2017.02.091>
 47. Jeffery GH, Bassett J, Mendham J, Denney RC (1989) Vogel's textbook of quantitative chemical analysis, 5th edn. New York 696. [https://doi.org/10.1016/0160-9327\(90\)90087-8](https://doi.org/10.1016/0160-9327(90)90087-8)
 48. Sharma RK, Lalita (2011) Synthesis and characterization of graft copolymers of N-Vinyl-2-Pyrrolidone onto guar gum for sorption of Fe²⁺ and Cr⁶⁺ ions. *Carbohydr Polym* 83:1929–1936. <https://doi.org/10.1016/j.carbpol.2010.10.068>
 49. Lalita SAP, Sharma RK (2017) Selective sorption of Fe(II) ions over Cu(II) and Cr(VI) ions by cross-linked graft copolymers of chitosan with acrylic acid and binary vinyl monomer mixtures. *Int J Biol Macromol* 105:1202–1212. <https://doi.org/10.1016/j.ijbiomac.2017.07.163>
 50. Singha AS, Shama A, Thakur VK (2008) Pressure induced graft-copolymerization of acrylonitrile onto Saccharum cilliare fibre and evaluation of some properties of grafted fibre. *Bull Mater Sci* 31:7–13. <https://doi.org/10.1007/s12034-008-0002-8>
 51. Luo MT, Li HL, Huang C, Zhang HR, Xiong L, Chen XF, Chen XD (2018) Cellulose-based absorbent production from bacterial cellulose and acrylic acid: synthesis and performance. *Polymers (Basel)*. <https://doi.org/10.3390/polym10070702>
 52. Huacai G, Wan P, Dengke L (2006) Graft copolymerization of chitosan with acrylic acid under microwave irradiation and its water absorbency. *Carbohydr Polym* 66:372–378. <https://doi.org/10.1016/j.carbpol.2006.03.017>
 53. Mukherjee A, Halder S, Datta D, Anupam K, Hazra B, Kanti Mandal M, Halder G (2017) Free radical induced grafting of acrylonitrile on pre-treated rice straw for enhancing its durability and flame retardancy. *J Adv Res* 8:73–83. <https://doi.org/10.1016/j.jare.2016.12.003>
 54. French AD (2014) Idealized powder diffraction patterns for cellulose polymorphs. *Cellulose* 21:885–896. <https://doi.org/10.1007/s10570-013-0030-4>
 55. Park S, Baker JO, Himmel ME, Parilla PA, Johnson DK (2010) Cellulose crystallinity index: measurement techniques and their impact on interpreting cellulase performance. *Biotechnol Biofuels* 3: 10. <https://doi.org/10.1186/1754-6834-3-10>
 56. Kumar R, Sharma RK, Singh AP (2018) Grafted cellulose: a bio-based polymer for durable applications. *Polym Bull* 75:2213–2242. <https://doi.org/10.1007/s00289-017-2136-6>
 57. Kumar R, Sharma RK, Singh AP (2017) Cellulose based grafted biosorbents-journey from lignocellulose biomass to toxic metal ions sorption applications-a review. *J Mol Liq* 232:62–93
 58. Konicki W, Aleksandrak M, Mijowska E (2017) Equilibrium, kinetic and thermodynamic studies on adsorption of cationic dyes from aqueous solutions using graphene oxide. *Chem Eng Res Des* 123:35–49. <https://doi.org/10.1016/j.cherd.2017.03.036>
 59. Langmuir I (1918) The adsorption of gases on plane surfaces of glass, mica and platinum. *J Am Chem Soc* 40:1361–1403. <https://doi.org/10.1021/ja02242a004>
 60. Rahman N, Haseen U (2014) Equilibrium modeling, kinetic, and thermodynamic studies on adsorption of Pb(II) by a hybrid inorganic-organic material: polyacrylamide zirconium(IV) iodate. *Ind Eng Chem Res* 53:8198–8207. <https://doi.org/10.1021/ie500139k>
 61. Kumar V, Rehani V, Kaith BS, Saruchi (2018) Synthesis of a biodegradable interpenetrating polymer network of Av-cl-poly(AA-ipn-AAm) for malachite green dye removal: kinetics and thermodynamic studies. *RSC Adv* 8:41920–41937. <https://doi.org/10.1039/c8ra07759b>
 62. Crini G, Peindy HN, Gimbert F, Robert C (2007) Removal of C.I. basic green 4 (malachite green) from aqueous solutions by adsorption using cyclodextrin-based adsorbent: kinetic and equilibrium studies. *Sep Purif Technol* 53:97–110. <https://doi.org/10.1016/j.seppur.2006.06.018>

63. Saruchi KV, Rehani V, Kaith BS (2018) Microwave-assisted synthesis of biodegradable interpenetrating polymer network of aloe vera–poly(acrylic acid-co-acrylamide) for removal of malachite green dye: equilibrium, kinetics and thermodynamic studies. *Iran Polym J (English Ed)* 27:913–926. <https://doi.org/10.1007/s13726-018-0665-y>
64. Naseeruteen F, Hamid NSA, Suah FBM, Ngah WSW, Mehamod FS (2018) Adsorption of malachite green from aqueous solution by using novel chitosan ionic liquid beads. *Int J Biol Macromol* 107:1270–1277. <https://doi.org/10.1016/j.ijbiomac.2017.09.111>
65. Sharma AK, Priya KBS et al (2019) Selective removal of cationic dyes using response surface methodology optimized gum acacia-sodium alginate blended superadsorbent. *Int J Biol Macromol* 124:331–345. <https://doi.org/10.1016/j.ijbiomac.2018.11.213>
66. Gündüz F, Bayrak B (2017) Biosorption of malachite green from an aqueous solution using pomegranate peel: equilibrium modelling, kinetic and thermodynamic studies. *J Mol Liq* 243:790–798. <https://doi.org/10.1016/j.molliq.2017.08.095>
67. Gopi S, Pius A, Thomas S (2016) Enhanced adsorption of crystal violet by synthesized and characterized chitin nano whiskers from shrimp shell. *J Water Process Eng* 14:1–8. <https://doi.org/10.1016/j.jwpe.2016.07.010>
68. Sharma AK, Priya KBS et al (2019) Efficient capture of eosin yellow and crystal violet with high performance xanthan-acacia hybrid super-adsorbent optimized using response surface methodology. *Colloids Surf B Biointerfaces* 175:314–323. <https://doi.org/10.1016/j.colsurfb.2018.12.017>
69. Baghdadi M, Jafari A, Pardakhti A (2016) Removal of crystal violet from aqueous solutions using functionalized cellulose microfibers: a beneficial use of cellulosic healthcare waste. *RSC Adv* 6:61423–61433. <https://doi.org/10.1039/C6RA08901A>
70. Ahmad R (2009) Studies on adsorption of crystal violet dye from aqueous solution onto coniferous pinus bark powder (CPBP). *J Hazard Mater* 171:767–773. <https://doi.org/10.1016/j.jhazmat.2009.06.060>
71. Krishnani KK, Meng X, Christodoulatos C, Boddu VM (2008) Biosorption mechanism of nine different heavy metals onto biomatrix from rice husk. *J Hazard Mater* 153:1222–1234. <https://doi.org/10.1016/j.jhazmat.2007.09.113>
72. Asuquo ED, Martin AD (2016) Sorption of cadmium (II) ion from aqueous solution onto sweet potato (*Ipomoea batatas* L.) peel adsorbent: characterisation, kinetic and isotherm studies. *J Environ Chem Eng* 4:4207–4228. <https://doi.org/10.1016/j.jece.2016.09.024>
73. Li Y, Du Q, Liu T et al (2012) Equilibrium, kinetic and thermodynamic studies on the adsorption of phenol onto graphene. *Mater Res Bull* 47:1898–1904. <https://doi.org/10.1016/j.materresbull.2012.04.021>
74. Wang C, Wang H, Gu G (2018) Ultrasound-assisted xanthation of cellulose from lignocellulosic biomass optimized by response surface methodology for Pb(II) sorption. *Carbohydr Polym* 182:21–28. <https://doi.org/10.1016/j.carbpol.2017.11.004>
75. Wang C, Wang H (2018) Pb(II) sorption from aqueous solution by novel biochar loaded with nano-particles. *Chemosphere* 192:1–4. <https://doi.org/10.1016/j.chemosphere.2017.10.125>
76. Wang C, Wang H, Cao Y (2018) Pb(II) sorption by biochar derived from *Cinnamomum camphora* and its improvement with ultrasound-assisted alkali activation. *Colloids Surf A Physicochem Eng Asp* 556:177–184. <https://doi.org/10.1016/j.colsurfa.2018.08.036>
77. Abdelhafez AA, Li J (2016) Removal of Pb(II) from aqueous solution by using biochars derived from sugar cane bagasse and orange peel. *J Taiwan Inst Chem Eng* 61:367–375. <https://doi.org/10.1016/j.jtice.2016.01.005>
78. Elgueta E, Sánchez J, Dax D, Xu C, Willför S, Rivas BL, González M (2016) Functionalized galactoglucomannan-based hydrogels for the removal of metal cations from aqueous solutions. *J Appl Polym Sci* 133:44093. <https://doi.org/10.1002/app.44093>
79. Zhang M, Li Y, Yang Q, Huang L, Chen L, Ni Y, Xiao H (2018) Temperature and pH responsive cellulose filament/poly (NIPAM-co-AAc) hybrids as novel adsorbent towards Pb(II) removal. *Carbohydr Polym* 195:495–504. <https://doi.org/10.1016/j.carbpol.2018.04.082>

Publisher's note Springer Nature remains neutral with regard to jurisdictional claims in published maps and institutional affiliations.